BMC Plant Biology

RESEARCH

Open Access

Integrative analysis of transcriptome and metabolome reveal molecular mechanism of tolerance to salt stress in rice

Rui Deng[1,2†], Yao Li[1,2†], Nai-Jie Feng[1,2,3*], Dian-Feng Zheng[1,2,3*], Aaqil Khan[1,2], You-Wei Du[1,2], Jian-Qin Zhang[1,2], Zhi-Yuan Sun[1,2], Jia-Shuang Wu[1,2], Ying-Bin Xue[1,2] and Zi-Hui Huang[1,2]

Abstract

Background Salt stress is considered to be one of the major abiotic stresses influencing rice growth and productivity. To improve rice crop productivity in saline soils, it is essential to choose a suitable variety for mitigating salt stress and gain a deep understanding of the underlying mechanisms. The current study explored the salt tolerance mechanism of wild rice '*HD96-1* (salt resistive)' and conventional rice '*IR29* (salt sensitive)' by evaluating morph-physiological, transcriptomic, and metabolomic approaches.

Results Physiological data indicated that *HD96-1* had higher chlorophyll content, higher photosynthetic efficiency, more stable Na^+/K^+, less H_2O_2, and lower electrolyte leakage under salt stress compared with *IR29*. Transcriptomic and metabolomic data showed that the expression of *NHXs* in *IR29* was significantly down-regulated under salt stress, leading to a large accumulation of Na^+ in the cytoplasm, and that the expression of *CHLH*, *PORA*, and *PORB* was significantly down-regulated, inhibiting chlorophyll synthesis. *HD96-1* maintained the balance of Na^+ and K^+ by increasing the expression of *NHX4*, and there was no significant change in the expression of genes related to chlorophyll synthesis, which made *HD96-1* more resistant to salt stress than *IR29*. In addition, *HD96-1* inhibited the excessive synthesis of hydrogen peroxide (H_2O_2) and alleviated oxidative damage by significantly down-regulating the expression of *ACX4* under salt stress. *HD96-1* promoted the accumulation of isoleucine by up-regulating genes of branched-chain amino acid aminotransferase 2 and branched-chain amino acid aminotransferase 4 and might promote the synthesis of raffinose and stachyose by up-regulating the expression of the gene for galactitol synthase 2, which, in turn, maintained a stable osmotic pressure and relieved osmotic stress. We also found that *IR29* and *HD96-1* alleviated the inhibition of photosynthesis by salt stress by down-regulating the expression of light-harvesting chromophore protein complex (LHCH II)-related genes and reducing the excessive accumulation of glucose

†Rui Deng and Yao Li contributed equally to this work as co-first authors.

*Correspondence:
Nai-Jie Feng
fengnj@gdou.edu.cn
Dian-Feng Zheng
zhengdf@gdou.edu.cn

Full list of author information is available at the end of the article

metabolites, respectively. In addition, *HD96-1* enhances salt tolerance by regulating *C2H2* and *bHLH153* transcription factors.

Conclusion Under salt stress, *HD96-1* maintained ionic balance and photosynthetic efficiency by up-regulating the expression of *NHX4* gene and reducing the overaccumulation of glucose metabolites, respectively, and mitigated osmotic stress and oxidative stress by down-regulating the expression of *ACX4* and promoting the accumulation of isoleucine, respectively, thereby enhancing the adaptability to salt stress. *IR29* maintained photosynthetic efficiency under salt stress by down-regulating the expression of light-harvesting chromophore protein complex (LHCH II)-related genes, thereby enhancing adaptation to salt stress.

Keywords Rice, Salt stress, Transcriptome, Metabolome, Photosynthesis

Introduction

Salt stress is a vital environmental problem that seriously influence the plant growth and development [1, 2]. Currently, about 950 million hectares of arable cropland including 250 million hectares irrigated land are affected by salt stress [2]. Salt stress cause hazardous impacts to plants such as ionic, osmotic, and oxidative stress, which retards normal plant growth and development [3, 4]. Exposed to salt stress, plants have the ability to evolved a complex set of adaptive mechanisms [5]. In response to environmental stresses, many plants influence morphology, physiology or metabolites by altering transcript levels [6, 7]. Previous study reported that Sesame promotes ABA biosynthesis by significantly upregulating the expression of genes related to the control of 9-cis-epoxycarotenoid dioxygenases, thereby improving salt tolerance in sesame [8]. Kale improves its antioxidant capacity by increasing the expression of superoxide dismutase (SOD), catalase (CAT), ascorbate peroxidase (APX), and ascorbate oxidase (AAO) genes, which ultimately improves the resistance of kale to drought stress [9]. Oilseed rape significantly increased the sugar content by increasing the expression of UDP glucose 6-dehydrogenase under cold stress, thus improving the adaptability of oilseed rape to cold stress [10].

Rice (*Oryza sativa* L.), staple food for more than 50% of the global population. Rice is moderately salt-sensitive crop [11, 12]. Salt stress inhibits rice morph-physiological traits and ultimately reduce grain yield and quality [13–16]. Salt stress limits plant growth mainly through ion toxicity and inhibition of photosynthesis [17]. Ion toxicity is usually due to excess input of Na^+ under salt stress, resulting in Na^+ accumulation in the cytoplasm [18]. Rice plant contains nine high-affinity K^+ transporter (*HKT*) genes encoding Na^+/K^+ symporter, five *OsNHX* Na^+/H^+ antiporters, and *OsSOS1* Na^+/K^+ antiporter genes [19]. Among them, Na^+/H^+ reverse transporter proteins (*NHXs*) play a key role in intracellular Na^+ secretion and zonal compartmentalization of Na^+ in vesicular membranes, which are essential for improving plant salt tolerance [20]. Under salt stress, the stomata of leaves close to reduce the transpiration and the intercellular CO_2 concentration [21]. Salt stress disrupts the lamellar structure of chloroplast basal lamellae and reduces the content of chlorophyll and carotenoids in leaves [22]. Salt stress also induced photoinhibition of PSII, and significantly reduced the maximum quantum yield (F_v / F_m) of PSII [23]. In response to salt stress, rice has developed complex adaptive mechanisms through long-term evolution, such as osmoregulation, selective ion uptake and rejection, compartmentalization of toxic ions, regulation of photosynthesis and energy metabolism [3, 24].

The introduction of sequencing technology has facilitated the use of transcriptome sequencing data to explore metabolic pathways associated with plant responses to salt stress and identify salt tolerance candidate genes. The mechanism of salt tolerance in rice has been explored using transcriptome sequencing technology [12]. Metabolomics has been widely used to study complex metabolites in plants under biotic and abiotic stresses, thus providing insights into a wide range of metabolic data and biaxial metabolic pathways [25]. By transcriptional-metabolic co-analysis, it was found that exogenous melatonin-treated soybeans control gene expression by up-regulating glycosidases and amino acid synthetases related to glycosidases [26]. This increased the activities of carbon and nitrogen metabolizing enzymes, thereby increasing the carbohydrate and amino acid contents and improving the resistance of soybean to drought stress [26]. Peach increased lignin content and improves its own resistance to cold stress by increasing the expression of lignin synthesis-related genes [27].

HD96-1 wild rice, often referred to as "seawater rice," is a salt-tolerant local variety that grows on coastal beaches or low-lying saline soils in Zhanjiang, China, where it is often inundated by seawater. It is characterized by resistance to pests and diseases, salt tolerance, and vigorous growth [25]. However, the regulatory molecular network of the *HD96-1* salt-tolerant gene remains unclear. Therefore, we selected salt-tolerant wild rice *HD96-1* and salt-sensitive *IR29* to explore the key salt-tolerant metabolic pathways and tap the salt-tolerant genes in wild rice *HD96-1*, which will provide a reference for breeders to develop new salt-tolerant varieties.

Results

Measurement of growth indicators

Salt stress significantly influenced the morphological traits of both varieties (Figs. 1 and 2). Salt stress markedly decreased the plant height, stem basal internode diameter, leaf area and above ground dry matter accumulation. Compared to CK, there were significantly corresponding percent decreased of 15.66% and 15.13% in plant height, 27.79% and 12.81% in stem basal internode diameter, 32.48% and 14.62% in leaf area, and 14.58% and 14.58% in above-ground dry matter, respectively at 2.5 and 4.5 leaf stages in *IR29* variety under salt stress. Compared to CK, there were significantly corresponding percent decreased of 26.77% and 15.03% in stem basal internode diameter, 22.48% and 4.23% in leaf area, and 8.51% and 35.94% in above-ground dry matter, respectively at 2.5 and 4.5 leaf stages in *HD96-1* variety under salt stress. In contrast to CK, the plant height of *HD96-1* slightly decreased under salt stress. Compared to CK, there were significantly corresponding percent decreased of 61.71% and 66.42% in total root length, 52.58% and 67.83% in total root surface, 40.05% and 69.15% in total root volume, and 39.04% and 51.73% in underground biomass, respectively at 2.5 and 4.5 leaf stages in *IR29* variety under salt stress. Compared to CK, there were significantly corresponding percent decreased of 59.23% and 51.51% in total root length, 55.08% and 53.17% in total root surface, 52.00% and 58.59% in total root volume, and 9% and 24.74% in underground biomass, respectively at 2.5 and 4.5 leaf stages in *HD96-1* variety under salt stress. These results indicated that *HD96-1* variety showed better performance under salt stress.

Effects of salt stress on Na^+ and K^+ contents and Na^+/K^+

Salt stress significantly increased leaf and root Na^+ content while significantly decreasing the K^+ in *IR29* and *HD96-1* compared to CK (Table 1). Compared to CK, the Na^+ content significantly increase was 12.85 folds and 11.27 folds in leaf, 3.98 folds and 3.02 folds in root, and K^+ content decreased by 0.03 folds and 0.15 folds in leaf and 0.14 folds and 0.15 folds in root, respectively, for *IR29* and *HD96-1* under salt stress. Compared to CK, salt stress significantly increased the leaf Na^+/K^+ ratios by 13.10 folds and 13.41 folds in leaf, and 4.81 folds and 3.75 folds in root, respectively, for *IR29* and *HD96-1*. The Na^+ content and Na^+/K^+ in the roots and leaves of *IR29* were higher than those of *HD96-1* under salt stress (Table 1). Compared with *HD96-1* wild rice, salt stress accumulated higher Na^+ content in the roots and leaves of *IR29* and inhibited K^+ uptake in *IR29*.

Effect of salt stress on photosynthetic pigments, gas exchange and chlorophyll fluorescence parameters in rice

Photosynthetic pigments of *IR29* and *HD96-1* were significantly decreased under salt stress (Fig. 3A, B, C). and the chlorophyll a, chlorophyll b, and carotenoid contents of *IR29* rice under S treatment were significantly decreased by 22.35%, 26.42%, and 20.92% at the two-leaf-one-heart stage and significantly decreased by 18.39%, 22.68%, and 18.63% at the four-leaf-one-heart stage, when compared with the CK control group. The above indexes of salt stress treatment in *HD96-1* were slightly decreased at the two-leaf-one-center stage and significantly decreased by 19.7%, 39.87%, and 9% at the four-leaf-one-center stage compared with CK treatment. Compared with *IR29*, *HD96-1* showed a smaller decrease in photosynthetic pigments under salt stress.

The gas exchange parameters were all significantly reduced in rice under salt stress treatments compared to the CK treatment (Fig. 3D, E, F, G). Among them, Pn, Gs, Ci, and Tr were significantly decreased by 18.83%, 36.26%, 5.23%, and 34.12% at the 2.5 leaf stage and 22.98%, 31.5%, 9.66%, and 37.5% at the 4.5 leaf stage, respectively, in the salt treatment of IR29 as compared

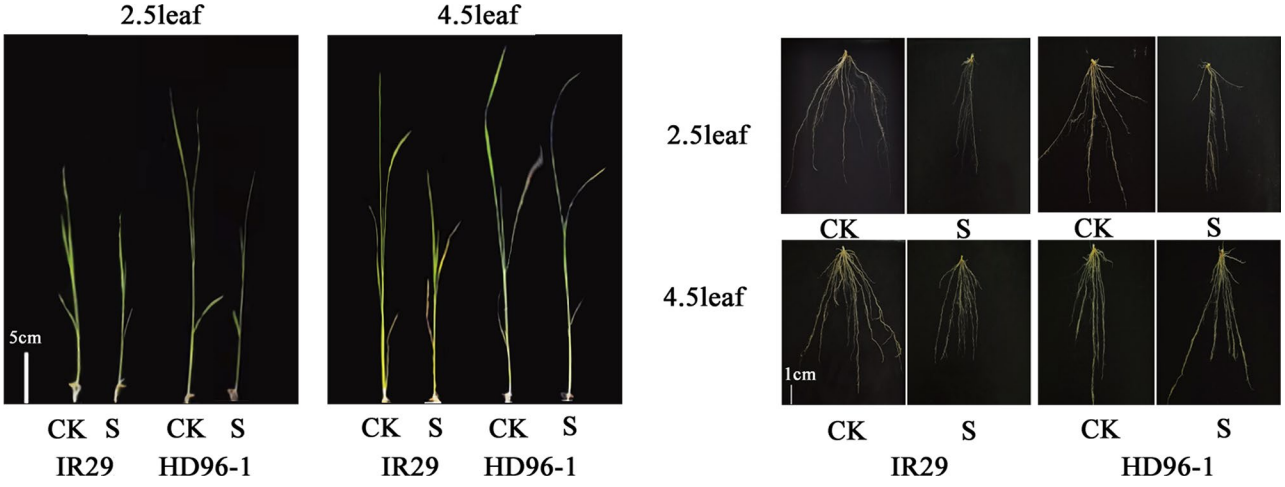

Fig. 1 Effects of salt stress on *IR29* and *HD96-1* phenotypes. CK:0 mM NaCl, S: 50 mM NaCl

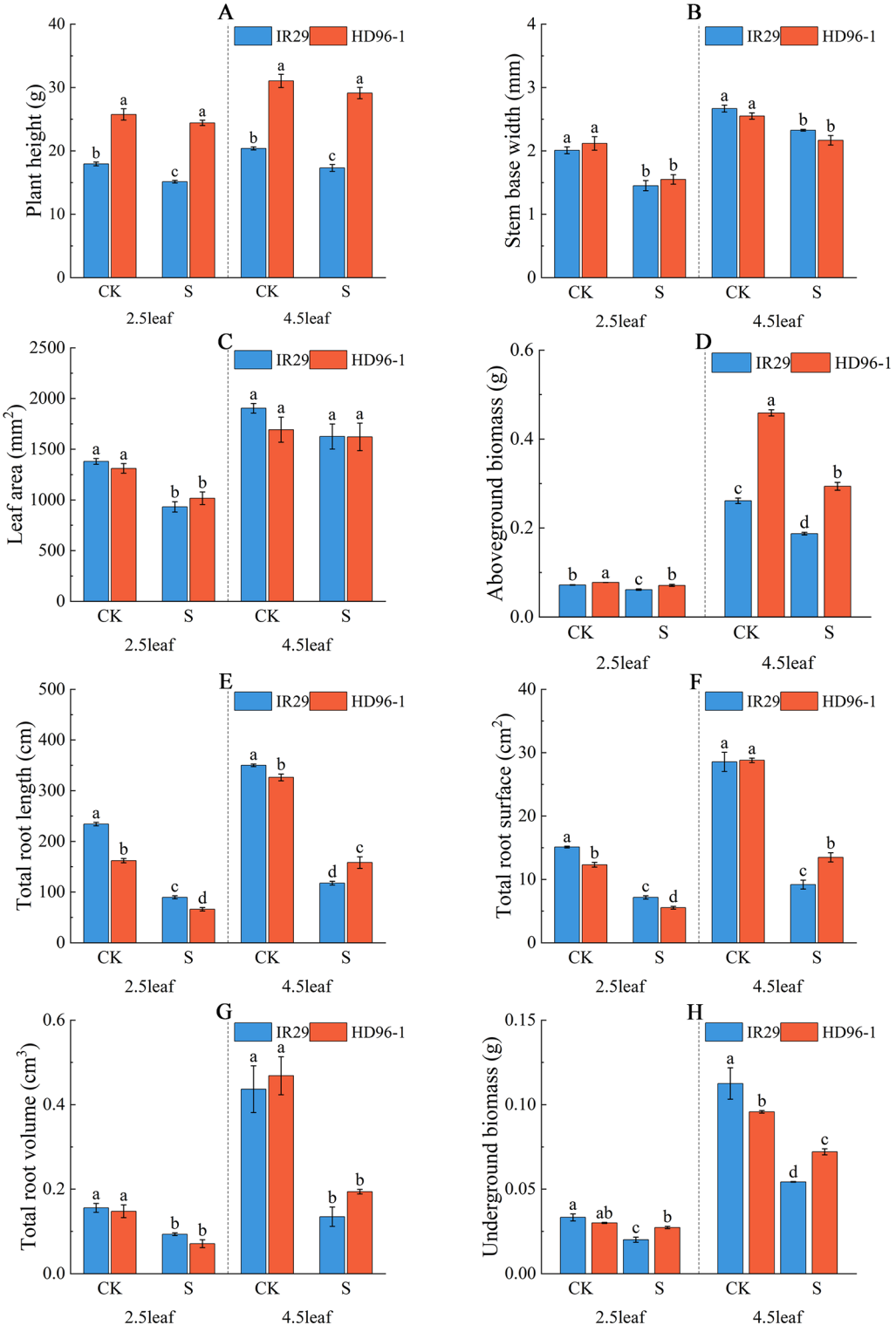

Fig. 2 Effect of salt stress on (**A**) plant height, (**B**) stem base width, (**C**) leaf area, (**D**) dry weight of aboveground parts, (**E**) total root length, (**F**) total root surface area, (**G**) total root volume, and (**H**) total root weight of *IR29* and *HD96-1*. CK:0 mM NaCl, S: 50 mM NaCl. Values are the mean ± SE of three replicate samples. Different letters in the data column indicate significant differences ($p < 0.05$) according to Duncan's test

Table 1 Effects of salt stress on Na^+ and K^+ contents and Na^+/K^+. CK:0 mM NaCl, S: 50 mM NaCl. Values are the mean ± se of three replicate samples. Different letters in the data column indicate significant differences ($p < 0.05$) according to Duncan's test

Treatment	Variety	Leaf Na^+	Leaf K^+	Leaf Na^+/K^+	Root Na^+	Root K^+	Root Na^+/K^+
CK	IR29	0.829 ± 0.001c	20.931 ± 0.112c	0.040 ± 0.000c	1.594 ± 0.002c	16.610 ± 0.000b	0.096 ± 0.000c
	HD96-1	0.846 ± 0.004c	29.324 ± 0.107a	0.029 ± 0.000d	1.597 ± 0.004c	16.618 ± 0.001a	0.096 ± 0.000c
S	IR29	11.484 ± 0.035a	20.351 ± 0.000d	0.564 ± 0.002a	7.944 ± 0.009a	14.229 ± 0.000c	0.558 ± 0.001a
	HD96-1	10.377 ± 0.021b	24.833 ± 0.116b	0.418 ± 0.002b	6.425 ± 0.005b	14.101 ± 0.000d	0.456 ± 0.000b

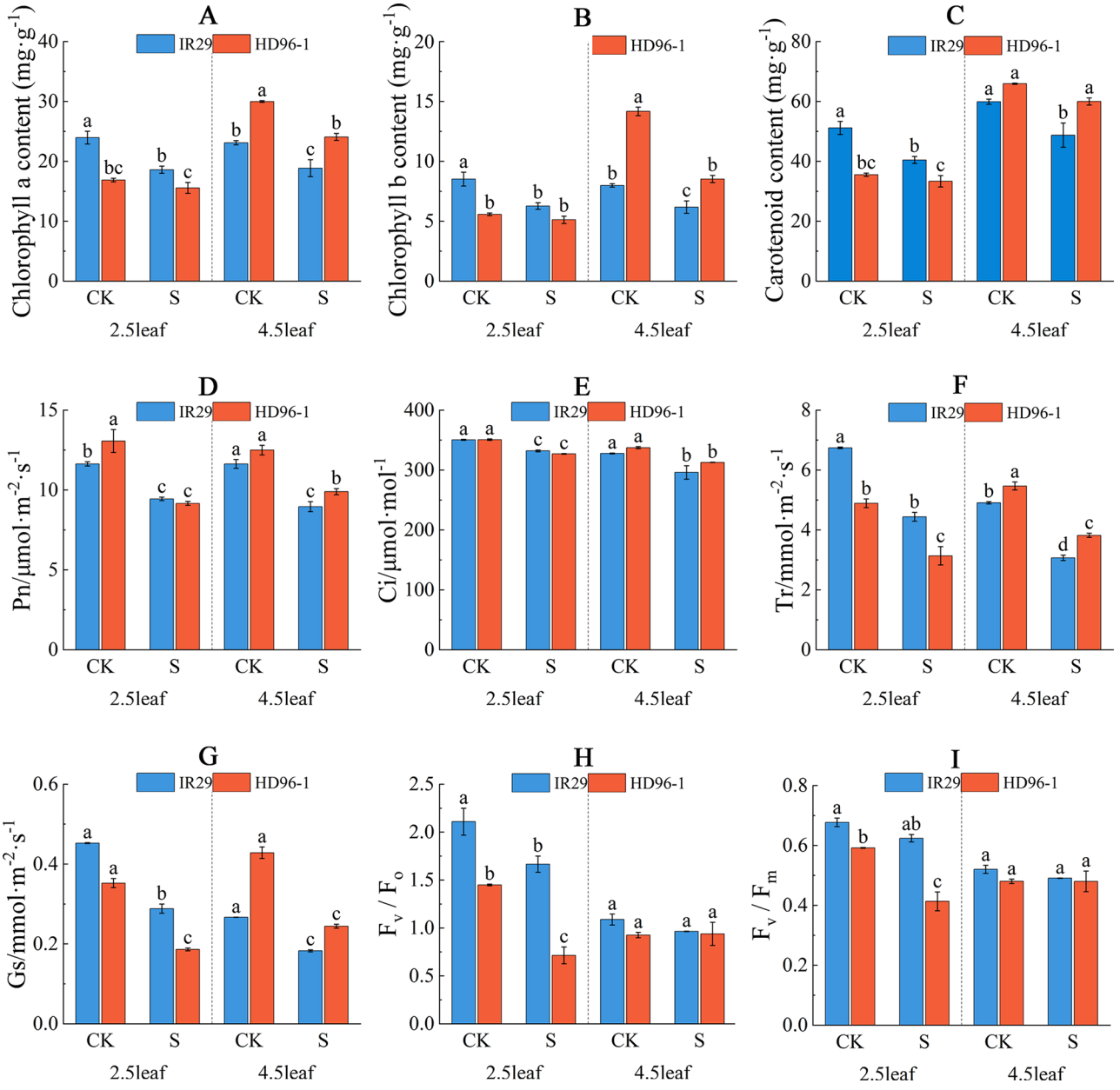

Fig. 3 Effects of salt stress on chlorophyll a content (**A**), chlorophyll b content (**B**), carotenoid content (**C**), net photosynthetic rate Pn (**D**), intercellular carbon dioxide concentration Ci (**E**), stomatal conductance Gs (**F**), transpiration rate Tr (**G**), quantum efficiency of PS II (**H**), and maximum quantum yield of PS II (**I**) in *IR29* and *HD96-1*. CK:0 mM NaCl, S: 50 mM NaCl. Values are the mean ± SE of three replicate samples. Different letters in the data column indicate significant differences ($p < 0.05$) according to Duncan's test

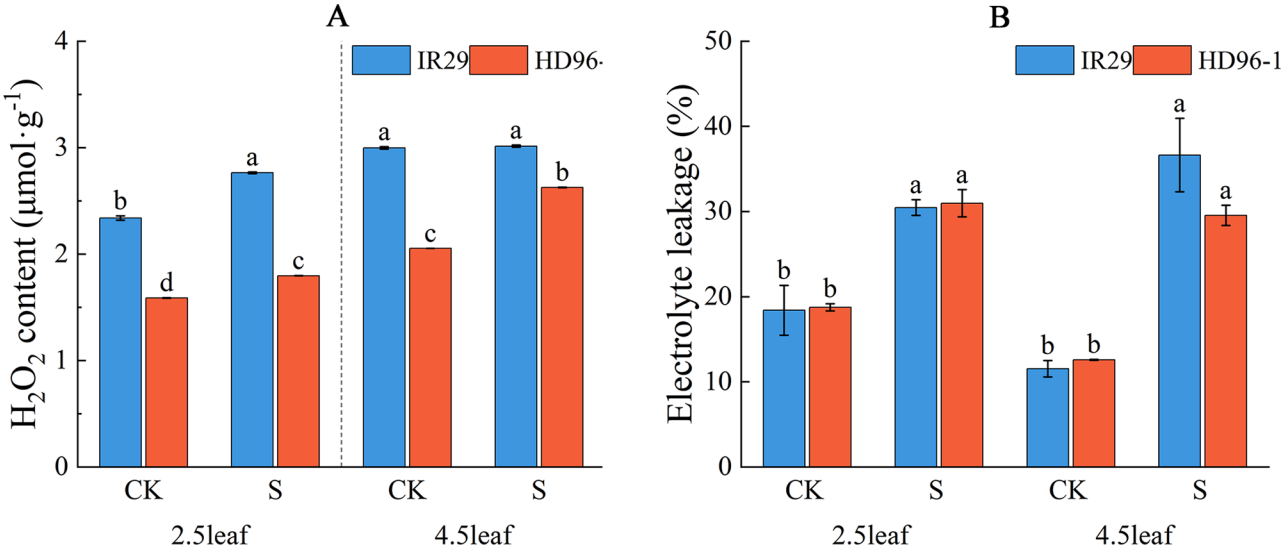

Fig. 4 Effects of salt stress on H_2O_2 content and electrolyte leakage in *IR29* and *HD96-1* rice. CK:0 mM NaCl, S: 50 mM NaCl. Values are the mean ± SE of three replicate samples. Different letters in the data column indicate significant differences ($p < 0.05$) according to Duncan's test

Table 2 Effect of salt stress on ABA content in *IR29* and *HD96-1*. Log2FC: log_2 fold change. Type: changes in ABA content

Index	Compounds	Class	Treatment	*P*-value	Fold Change	Log_2FC	Type
ABA	Abscisic acid	ABA	HS/HCK	0.96481	1.00136	0.00197	insig
			IS/ICK	0.00003	1.38610	0.47103	insig
ABA-GE	ABA-glucosyl ester	ABA	HS/HCK	0.90688	1.01529	0.02189	insig
			IS/ICK	0.23511	1.19538	0.25747	insig

with the CK treatment; The above indexes of salt stress treatment of *HD96-1* were significantly decreased by 29.87%, 47.11%, 6.75%, and 35.86% at the 2.5 leaf stage and 20.83%, 42.96%, 7.31%, and 30.12% at the 4.5 leaf stage as compared with CK treatment.

Fv/Fo (Fig. 3H) and Fv/Fm (Fig. 2I) of *IR29* rice in salt stress treatment significantly decreased by 21.05% and 7.83% at 2.5 leaf stage and 11.42% and 5.69% at 4.5 leaf stage, compared with CK treatment; Fv/Fo and Fv/Fm of *HD96-1* rice in salt stress treatment compared with CK control Compared with the CK control, Fv/Fo and Fv/Fm decreased significantly by 50.76% and 30.15% at the 2.5-leaf stage, and Fv/Fo increased by 1.30% and Fv/Fm decreased by 0.06% at the 4.5-leaf stage.

Effects of salt stress on the extent of cell membrane damage and antioxidant enzyme activities in rice cells

The cell membranes of both *IR29* and *HD96-1* were damaged to varying degrees under salt stress (Fig. 4A, B). At the 2.5 leaf stage, compared to the CK treatment, the S treatments significantly increased the content of H_2O_2 by 18.14% and 13.12%, and electrolyte leakage by 65.52% and 65.14%, respectively, for *IR29* and *HD96-1*. At the 4.5 leaf stage, compared to the CK treatment, the S treatments increased the content of H_2O_2 by 0.55% and 27.80%, and electrolyte leakage by 217.60% and 134.94%, respectively, for *IR29* and *HD96-1*. And we found that the H_2O_2 content in *IR29* rice was higher than that in *HD96-1* rice in both CK treatment and S treatment.

Effect of salt stress on ABA content in rice

|log2FC|≥1 and q value ≤ 0.05 were used as criteria for significant changes in hormone content. No significant changes in ABA and ABA-GE contents were observed in both *IR29* rice and *HD96-1* rice under salt stress (Table 2).

Response of rice transcriptome to salt stress

RNA sequences from 12 samples were analyzed (Additional table: S2). Each sample yielded an average size of approximately 6.70 GB of bases. The average Q30 was 89.9975%. Sequencing quality and library construction of the reaction samples were good, and data accuracy was high. Each sample was a clean read with reference to the genome sequence. These data met the criteria for subsequent analysis. In order to reflect the correlation of gene expression between samples, Pearson correlation coefficients were calculated for all gene expressions between each of the two samples, and these coefficients were reflected in the form of heatmaps. For all treatments, we can observe a high correlation between biological replicates, which indicates the reliability of biological replicates in this study (Supplementary file: Fig. 3). Principal Component Analysis (PCA) showed that PC1 captured

most of the variance in the data. PC2 captured less variance in the data (Supplementary file: Fig. 3). In addition, the PCA data showed good reproducibility within the same treatment and greater variability across treatments.

To verify the reliability of the RNA sequencing data, seven genes randomly selected from all treatments of the two *IR29*, *HD96-1*, were subjected to qRT-PCR analysis. qRT-PCR results showed a high degree of consistency between the up- and down-regulated changes in differential expression of the gene and the RNA sequencing data (Supplementary table: S1), proving that the RNA sequencing data were reliable.

Selection and functional characterization of differentially expressed genes in rice under salt stress

Gene expression was calculated and normalized by the TPM method, and|Log2FC|≥1 and q-value ≤ 0.05 significantly differentially expressed genes were selected. Compared with CK, there were 555 differentially expressed genes (331 up-regulated and 224 down-regulated) in *IR29* (IS/ICK) and 144 differentially expressed genes (21 up-regulated and 123 down-regulated) in *HD96-1* (HS/ICK) after salt stress (Fig. 5A, C). *IR29* and *HD96-1* had 60 common significant differentially expressed genes (Fig. 5A). These 60 genes had great differences in gene expression changes in *HD96-1* and *IR29* varieties after salt stress (Fig. 5D). Under salt stress, there were 495 unique differentially expressed genes in the *IR29* variety and 140 unique differentially expressed genes in *HD96-1* (Fig. 5A), and the changes in the expression of these differentially expressed genes varied considerably among the varieties (Fig. 5E, F).

KEGG annotation analysis of significantly differentially expressed genes under salt stress in the two varieties showed that all the differentially expressed genes in *HD96-1* and *IR29* under salt stress were mainly involved in several categories, including "carbohydrate metabolism", "amino acid metabolism", "energy metabolism", "signal transduction" etc. (Supplementary file: Fig. 1). Sixty genes were significantly differentially expressed in both rice species, representing the core genes associated with the salt stress response in rice. Among them, we found that the expression of the related control genes of senescence-specific cysteine protease SAG39 (*LOC107280424*, *OSNPB_030752500*) and galactinol synthase 2 (*LOC4344351*; *OSNPB_070687900*) was significantly elevated in both *HD96-1* and *IR29*, but the change in expression of *HD96-1* was significantly higher than *IR29*. Compared with CK, the expression of *bHLH153* transcription factor-related genes (*LOC4336261*, *OSNPB_040493100*), xyloglucan endotransglucosylase / hydrolase protein 24 (*LOC4341942*, *OSNPB_060696600*), and xyloglucan endotransglucosylase / hydrolase protein 25 (*LOC4341944*, *OSNPB_060697000*) in *HD96-1* was significantly reduced after salt stress (*LOC4341944*, *OSNPB_060697000*) showed a significant decrease in expression, and the corresponding genes of *IR29* showed a significant increase in expression. The related control gene for salt-stressed ABA 8'-hydroxylase, *CYP707A7* (*LOC4347261*), showed a significant down-regulation in *HD96-1* rice and a significant up-regulation in *IR29*. Among these core genes, a total of four transcription factors were identified, including *MYB*, *NAC*, *CO-like*, and *G2-like*, which have important regulatory roles in rice responses to salt stress (Supplementary table: S3). By GO enrichment analysis, 60 core genes were found to be involved in molecular functional processes such as aspartate kinase activity, xyloglucan: xyloglucosyl transferase activity, branched-chain amino acid aminotransferase activity, amino acid translocation, and other biological processes (Supplementary table: S4), and kegg enrichment analysis of these 60 core genes showed that the main significant enrichment was in the 2-oxocarboxylic acid metabolism, monobactam biosynthesis, lysine biosynthesis, biosynthesis of amino acids, cysteine and methionine, galactose metabolism, glycine, serine and threonine metabolism, glucosinolate biosynthesis, brassinosteroid biosynthesis, and mustard oleosin metabolic pathways (Fig. 6A, B; Supplementary table: S8).

The results showed that 495 genes were specifically and significantly differentially expressed only in *IR29* rice under salt stress compared with CK but did not show significant changes in *HD96-1*. Among them, the *LOC4333197* gene (*ZFP36*) was found to be significantly down-regulated 32.86-fold in *IR29* rice after salt stress, and the corresponding gene in *HD96-1* was not significantly changed (Supplementary table: S5). The *LOC9270505* gene was significantly down-regulated about 5-fold Supplementary table: S5) in *IR29* rice (*P0592B08.3*), and the expression of the corresponding gene in *HD96-1* was up-regulated, but not significantly. The GO functional enrichment analysis revealed that these 495 genes are involved in many processes of photosynthesis (Supplementary table: S6). To further understand the effects of salt stress on *IR29* rice and to further explore the mechanism of salt tolerance in *HD96-1*, we continued kegg analysis of these *IR29* rice-specific salt tolerance candidate genes. The results showed that these genes were significantly enriched in kegg pathways such as photosynthesis-antenna proteins, porphyrin and chlorophyll metabolism, and starch and sucrose metabolism (Fig. 6C, D; Supplementary table: S7). Among them, we focused on photosynthesis-antenna proteins, porphyrins, and chlorophyll metabolism and found that the expression of several genes on photosynthesis-antenna proteins showed a significant down-regulation (Supplementary table: S10), and several genes related to the control of chlorophyll a and chlorophyll b synthase on

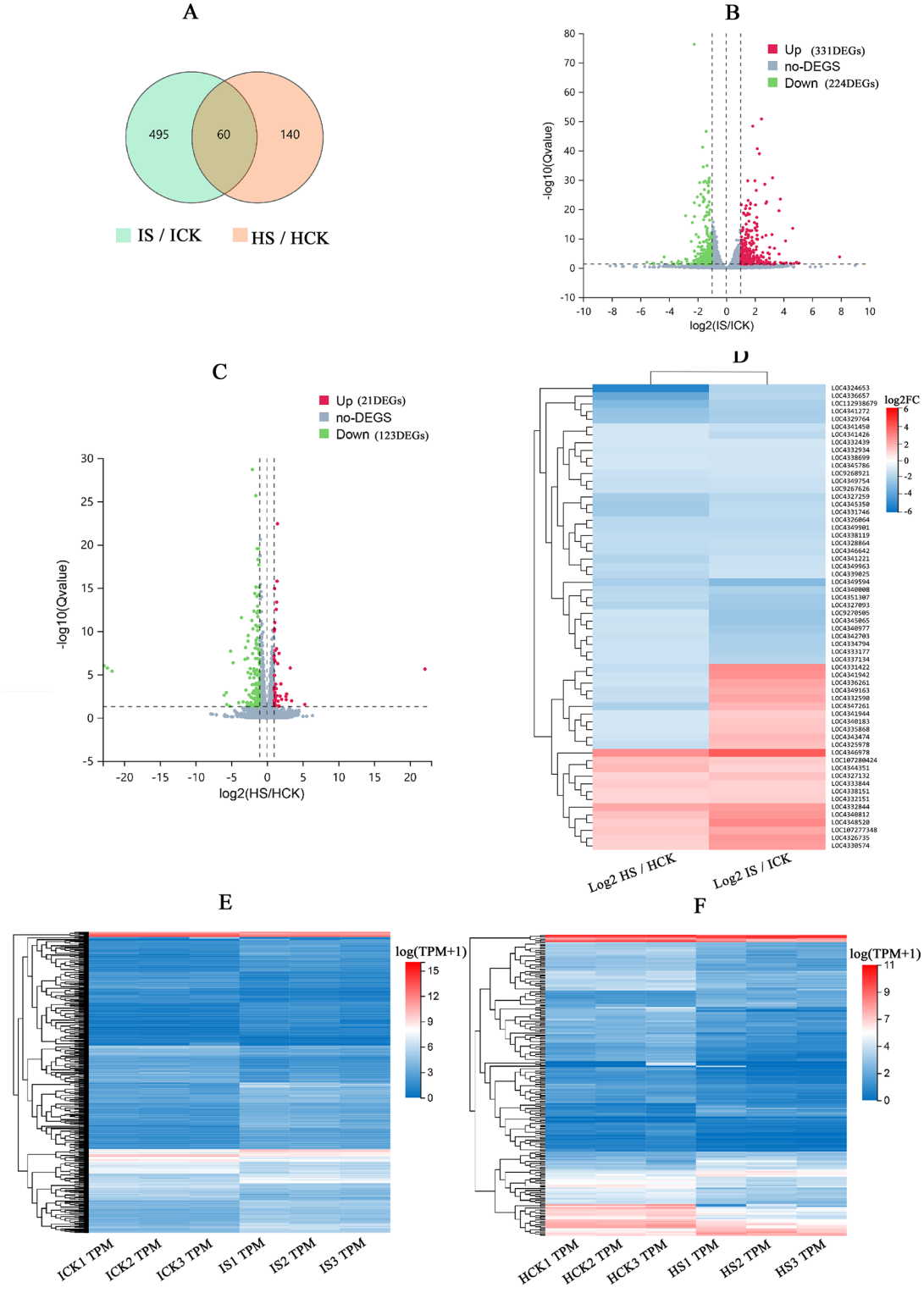

Fig. 5 Venn diagram of differentially expressed genes of *IR29* and *HD96-1* under salt stress (**A**), volcano diagram of up- and down-regulated genes of *IR29* (**B**) and *HD96-1* (**C**), heat map of clustering of common differentially expressed genes (**D**), and heat map of clustering of differentially expressed genes of *IR29* (**E**) and *HD96-1* (**F**) after salt stress

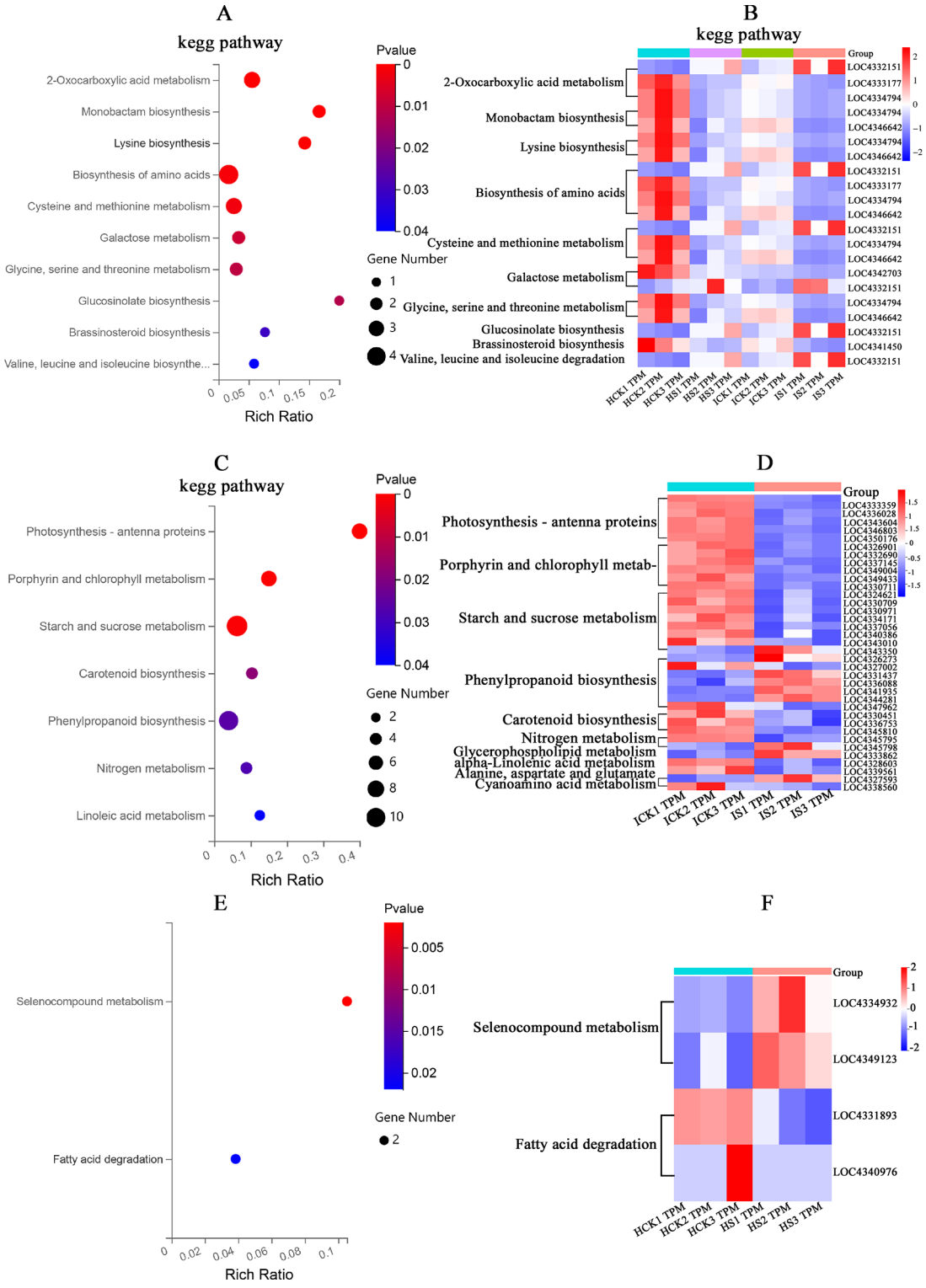

Fig. 6 Differentially expressed genes common to *HD96-1* and *IR29* (**A**), specific to *IR29* (**C**), and specific to *HD96-1* (**E**) were significantly enriched for the KEGG pathway under salt stress. Heatmap of gene expression of genes significantly enriched in the KEGG pathway under salt stress shared by *HD96-1* and *IR29* (**B**), *IR29*-specific (**D**), and *HD96-1*-specific (**F**)

the porphyrin-chlorophyll metabolism pathway showed a trend of down-regulation (Fig. 6D), which resulted in the inhibition of chlorophyll a and chlorophyll b synthesis, whereas no significant changes occurred in the expression of the relevant genes in *HD96-1* rice. In contrast, the expression of related genes did not change significantly in *HD96-1* rice. This suggests that higher salt sensitivity in *IR29* may be significantly linked to reduced photosynthetic efficiency. and that the greater resistance of *HD96-1* to salt stress may be due to the maintenance of the expression of the corresponding genes, thereby maintaining a more stable photosynthetic efficiency. There were 140 genes differentially expressed in *HD96-1* after salt stress. These 140 differentially expressed genes may be significantly associated with the salt tolerance of *HD96-1*. Kegg enrichment results showed that selenium compound metabolism and fatty acid degradation were significantly enriched (Fig. 6E, F). Multiple pathways such as starch and sucrose metabolic pathways, and amino acid biosynthesis were also enriched (Supplementary table: S9).

Response of rice metabolome to salt stress

The raw mass spectrometry data collected by LC-MS/MS and data processing were used to detect 13,652 differential metabolites in rice. VIP ≥ 1, Fold-Change ≥ 1.2, or ≤ 0.83 with a P-value < 0.05 were used as the screening criteria for differential metabolites. Compared with the control (CK), 100 and 187 metabolite contents were significantly changed in the IR29 and HD96-1 varieties, respectively, under salt stress. After salt stress, the accumulation of 46 metabolites was changed in both *IR29* and *HD96-1* (IS/ICK and HS/HCK), of which 29 metabolites were increased and 17 metabolites were decreased in IS/ICK, and 27 metabolites were increased and 19 metabolites were decreased in HS/HCK. There were 23 metabolites whose accumulation increased only in the IS/ICK group and 31 differential metabolites whose accumulation decreased only in the IS/ICK group, while 17 and 96 metabolites whose accumulation increased and decreased only in HS/HCK, respectively (Fig. 7A, B; Supplementary table: S11). Analysis of metabolite kegg enrichment pathways revealed that *HD96-1* differential metabolites under salt stress were mainly involved in the biosynthesis of amino acids, 2-oxocarboxylic acid metabolism, starch and sucrose metabolism, pantothenate and CoA biosynthesis, valine, leucine, and isoleucine biosynthesis, carbon fixation in photosynthetic organisms, arginine biosynthesis, and alanine, aspartic and glutamate metabolism, etc., suggesting that these metabolic pathways may play an important role in the adaptation of *HD96-1* to salt stress (Fig. 7C, D). Among them, the contents of L-isoleucine on the biosynthetic pathways of valine, leucine, and isoleucine were significantly up-regulated (Supplementary table: S12). The contents of glucose metabolites in the starch and sucrose metabolic pathways were significantly down-regulated (Supplementary table: S12).

Key biological pathways involved in transcriptomic and metabolomic changes

To better understand the changes in rice physiology under salt stress, we focused on the link between gene expression and metabolite changes before and after salt stress. Some genes encoding key enzymes are involved in the synthesis of key metabolites as well as degradation processes in rice, and these genes may be important for improving salt tolerance in rice. By kegg pathway enrichment analysis of significantly differentially expressed genes and differential metabolite products after salt stress. Within *IR29* varieties, 17 kegg pathways were significantly enriched by differential metabolites, including starch and sucrose metabolism (ko00500), lysine biosynthesis (ko00300), cysteine and methionine metabolism (ko00270), and Monobactam biosynthesis, which were significantly enriched by differentially expressed genes and differential metabolites (Fig. 8A). Within the *HD96-1* variety, eight kegg pathways were significantly enriched by differential metabolites, with 2-oxidative carboxylation showing significant enrichment in transcriptomic and metabolomic kegg pathway enrichment analyses (Fig. 8B). In all three significantly enriched kegg metabolic pathways, *IR29* amino acid biosynthesis (ko01230), 2-oxocarboxylic acid metabolism (ko01210), valine, leucine, and isoleucine biosynthesis (ko00290), and valine, leucine, and isoleucine degradation (ko00280), the levels of isoleucine were all trending significantly upward, and the isoleucine positively related branched-chain amino acid aminotransferase 2 (*LOC4332151*) expression all showed a significant up-regulation (Fig. 9). Based on transcriptome and metabolome analyses, it was found that the differentially expressed genes and differential metabolites of *HD96-1* rice showed significant enrichment in the 2-oxocarboxylic acid metabolism kegg pathway after salt stress, which was significantly increased in isoleucine content, and the expression of branched-chain amino acid aminotransferase 2 (*LOC4332151*), which is positively correlated with isoleucine, was also significantly up-regulated, which was consistent with the trend of the *IR29* rice in isoleucine and branched-chain amino acid transaminase 2 in *IR29* rice. Transcriptome and metabolome data showed that the differentially expressed genes and differential metabolites of *HD96-1* under salt stress were significantly enriched in both starch and sucrose metabolism pathways, with transcriptome data showing that β-glucosidase (β▪glucosidase, EC3.2.1. 21) was significantly up-regulated on this pathway, and metabolome data showed that starch and sucrose metabolism

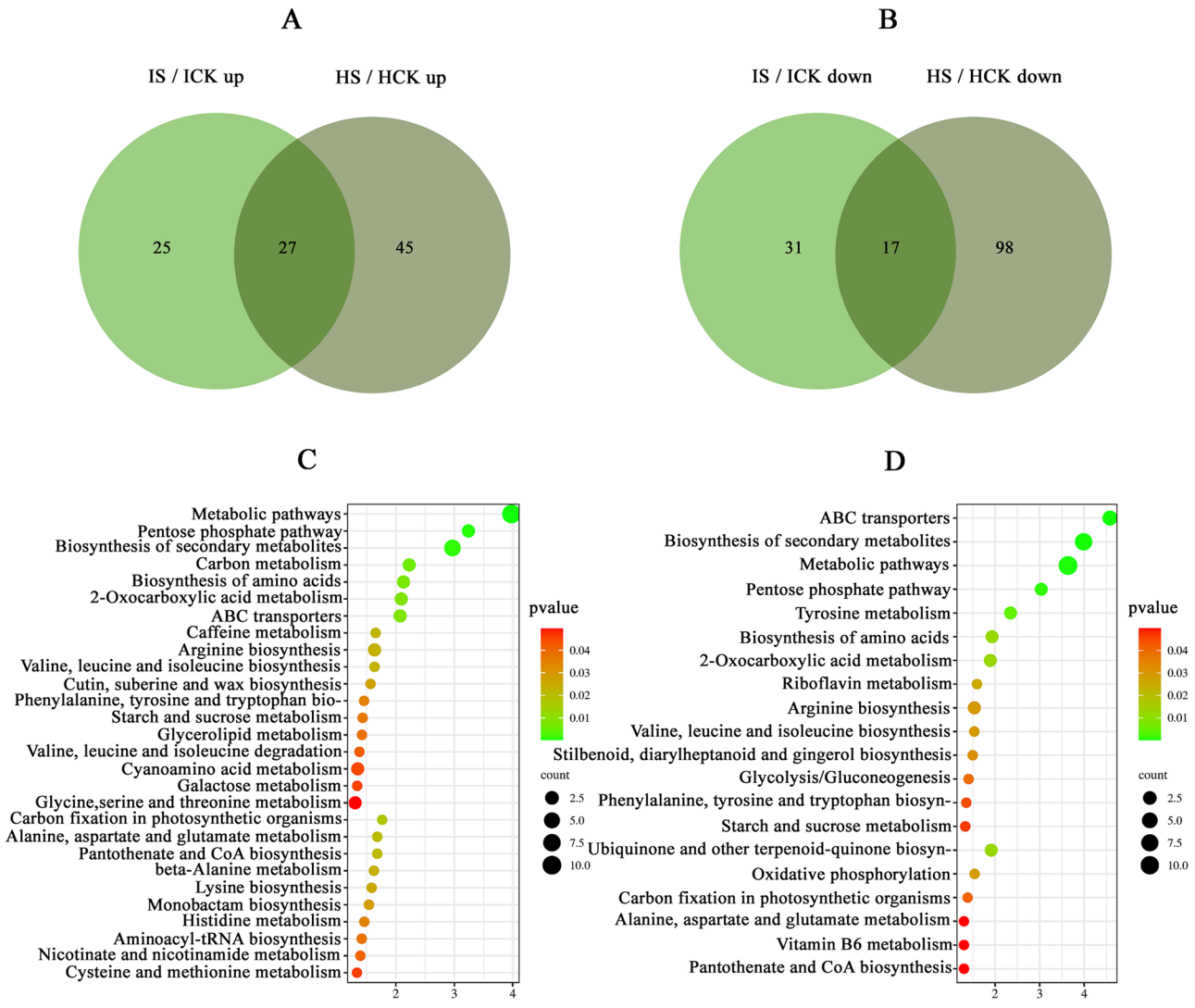

Fig. 7 Increase (**A**) and decrease (**B**) in *IR29* and *HD96-1* metabolites under salt stress Venn diagram. Differential metabolites of *IR29* (**C**) and *HD96-1* (**D**) were significantly enriched in the kegg pathway under salt stress

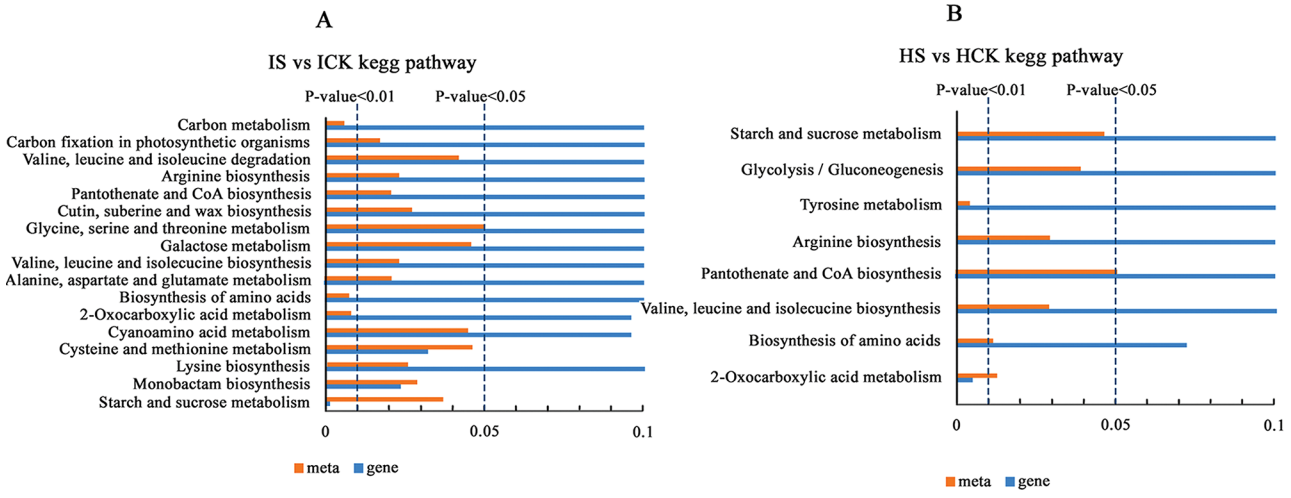

Fig. 8 Co-enrichment of the kegg pathway by differentially expressed genes and differential metabolites after salt stress in *IR29* (**A**) and *HD96-1* (**B**)

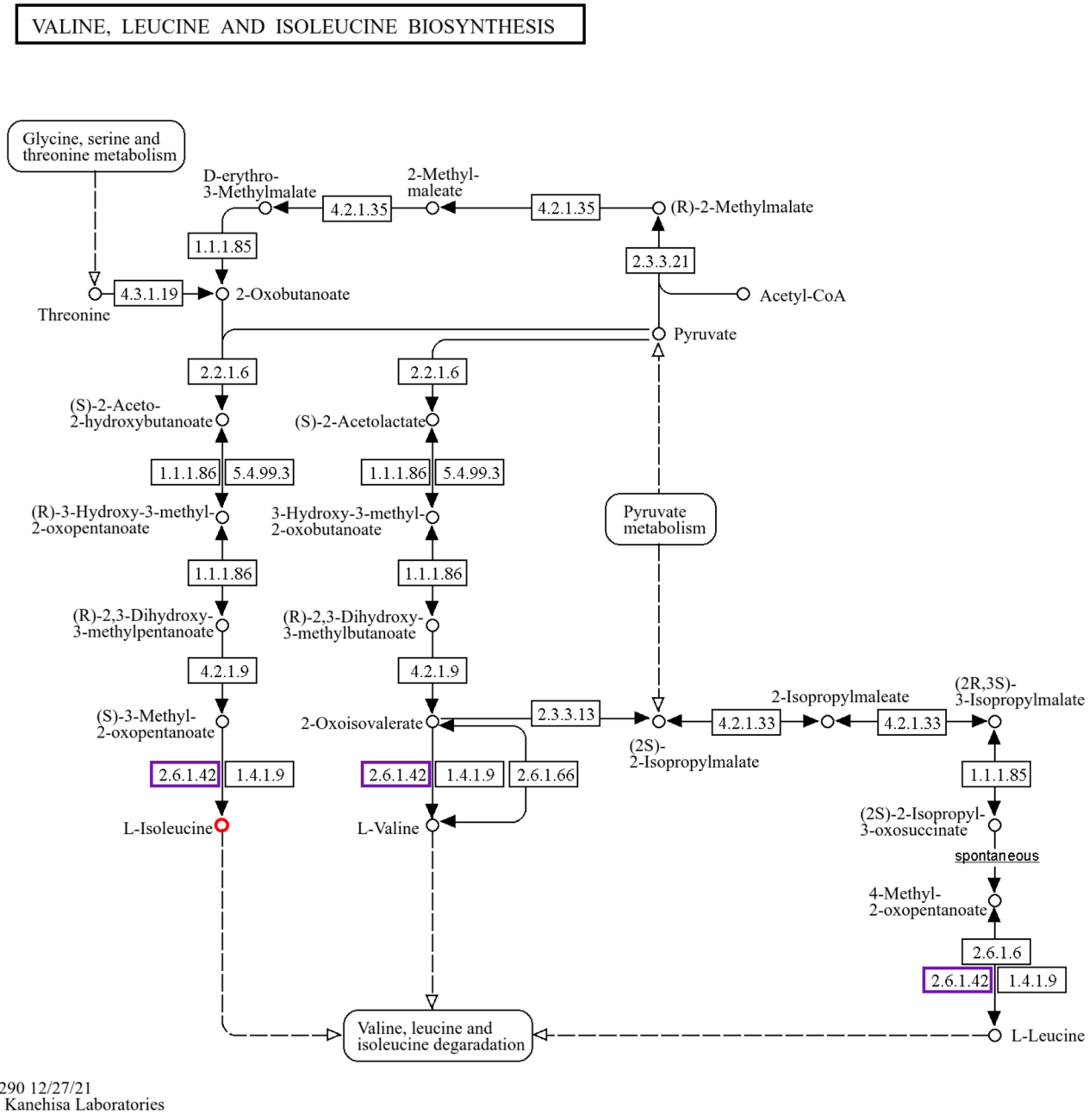

Fig. 9 A biosynthetic pathway for the co-enrichment of valine, leucine and isoleucine by *HD96-1* differential genes and differential metabolites under salt stress

pathways were significantly enriched and glucose content on this pathway was significantly decrease (Fig. 10).

Discussion

Salt stress leads to the waste of a large amount of land resources and also caused huge economic losses globally [28]. Therefore, improving salt tolerance in rice is important for solving the problem of food security. In this study, through the transcriptome, metabolome, morph-physiological characteristics, we deeply investigated the salt tolerance mechanism of the *HD96-1* rice variety under salt stress considering key related genes, and important metabolites of salt stress [29].

Effect of salt stress on photosynthesis metabolism of rice

Previous studies have demonstrated that salt stress causes a decrease in photosynthetic efficiency and inhibits plant growth by reducing chlorophyll content, decreasing photosynthetic gas exchange parameters, and producing photoinhibition [30, 31]. The present study is consistent

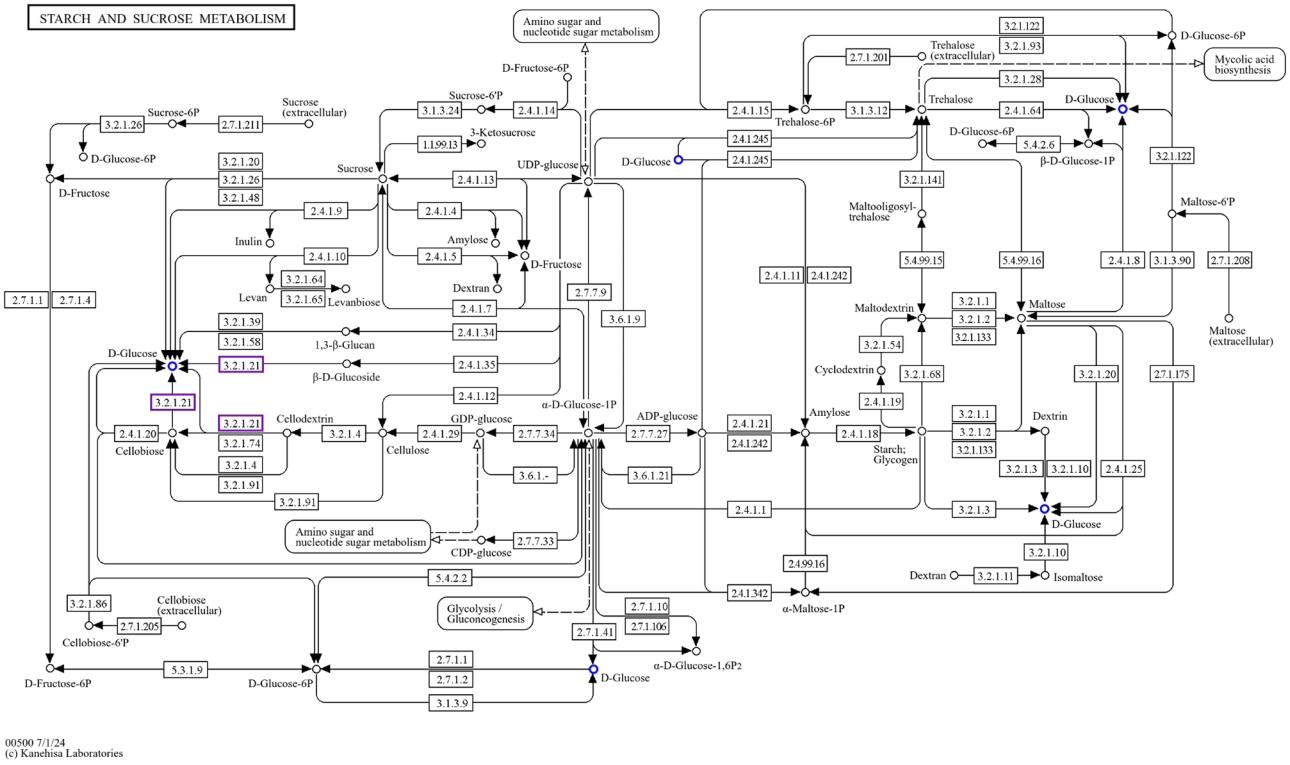

Fig. 10 *HD96-1* differential genes and differential metabolites co-enrich starch and sucrose metabolic pathways under salt stress

with previous studies [30]. Previous studies showed that under salt stress, various plants species have the ability to improve photosynthetic efficiency by increasing photosynthetic pigments, carbon metabolism, or decreasing the photoinhibition index [29, 32]. The expression of *CHLH*, *PORA*, and *PORB* were significantly down-regulated in *IR29* after salt stress, and these enzymes positively regulated chlorophyll synthesis [33, 34]. Magnesium chelatase (CHLH) promotes the insertion of Mg^{2+} into protoporphyrin during chlorophyll synthesis [35]. During light, *PORA* transient expression promotes chlorophyll synthesis, and *PORB* was present for long periods of time throughout plant development and promotes the synthesis of large amounts of chlorophyll [34, 36]. Under salt stress, the expression of several related control genes of chlorophyll a and chlorophyll b synthase of *IR29* was significantly down-regulated (Supplementary table: S4), which inhibited the synthesis of chlorophyll a and chlorophyll b, and ultimately reduced the photosynthetic efficiency [37]. The expression of several related control genes of chlorophyll a and chlorophyll b synthase of *HD96-1* did not undergo significant changes.

The chlorophyll fluorescence index, Fv/Fm, was utilized as a photoinhibition index to reflect the efficiency of light energy conversion in PSII active centers [38]. In this study, the Fv/Fm of *IR29* under salt stress was lower than that of *HD96-1* under salt stress. These results indicated that salt stress affected PSII of *IR29* more severely than *HD96-1*. The light-harvesting pigment-protein complex (LHCH II) of photosystem II is mainly composed of six pigment-protein complexes, which are formed by proteins and pigments encoded by six genotypes, namely, *Lhcb1*, *Lhcb2*, *Lhcb3*, *Lhcb4*, *Lhcb5*, and *Lhcb6*, respectively [39, 40]. Previous studies had demonstrated that grapevine protects itself from salinity stress by significantly down-regulating LHCHII-related genes, reducing light energy uptake by the light-harvesting pigment protein complexes, and mitigating photoinhibition in order to protect grape plants under salinity stress [41, 42]. *IR29* in this study alleviated photoinhibition by significantly down-regulating *Lhcb* expression (Supplementary file: S5) after salt stress, which is in agreement with the results of previous studies [43]. Corresponding gene expression of *HD96-1* showed non-significant changes. These also proved that under salt stress, *HD96-1* showed lower photoinhibition, less impaired photochemical conversion efficiency of the PSII protein complex, higher chlorophyll content, and higher photosynthetic efficiency, which ultimately resulted in higher salt tolerance for *HD96-1* [44].

Low concentrations of glucose stimulate plant growth and high concentrations of glucose inhibit growth by inhibiting photosynthesis in plants [45, 46]. The large amount of sugar accumulated in plants under salt stress also inhibits normal photosynthesis and slows plant growth [46]. Previous studies have shown that ethylene alleviates the inhibition of photosynthesis by salt

stress by reducing the sensitivity of plants to glucose [47]. In this study, the content of glucose metabolites on the starch and sucrose metabolic pathways of *HD96-1* decreased significantly under salt stress, thus alleviating the inhibition of *HD96-1* photosynthesis by salt stress, which is consistent with the results of previous studies [47, 48], but the specific regulatory mechanisms still need to be further explored. In addition, the genes related to the control of β-glucosidase (EC 3.2.1. 21) on starch and sucrose metabolic pathways were significantly up-regulated. Previous studies demonstrated that β-glucosidase plays an important role in plant resistance to salt stress [49]. β-glucosidase is inhibited by the reaction product glucose [50]. The glucose content of *HD96-1* was significantly decreased under salt stress, and the inhibitory effect on β-glucosidase was weakened, so the gene expression of β-glucosidase was significantly up-regulated, which ultimately improved the tolerance of *HD96-1* rice to salt stress. However, the specific regulatory mechanism of β-glucosidase in *HD96-1* rice to salt stress is not clear and still needs to be further explored. β-glucosidase in *IR29* rice did not undergo the relevant response under salt stress.

Effect of salt stress on antioxidant metabolism of rice

Prolonged salt stress leads to oxidative stress injury through excessive ROS production by plants [51]. *ACX4* (acyl-CoA oxidase) is the rate-limiting enzyme in the peroxisomal β-oxidation pathway encoding ultra-long-chain fatty acids and a major producer of H_2O_2 [52, 53]. The results of transcriptome studies showed that the related control genes (*LOC4340976*; *OSNPB_060347100*; *ACX4*) of HD96-1 acyl-coenzyme A oxidase 4(*ACX4*) showed a significant decreasing trend under salt stress, and there was no significant change in the expression of peroxisome-related control genes in *IR29* rice. The results of physiological studies showed that the H_2O_2 content of *HD96-1* was significantly lower than that of *IR29* under salt stress. We suggest that *HD96-1* inhibits hydrogen peroxide (H_2O_2) synthesis and prevents oxidative damage caused by excessive accumulation of H_2O_2 by down-regulating the expression of *ACX4* [54].

Effect of salt stress transcription factors of rice

The expression of the *bHLH153* transcription factor-related gene (*LOC4336261*, *OSNPB_040493100*) of *HD96-1* was significantly decreased, and the expression of the corresponding gene of *IR29* was significantly increased under salt stress. *bHLH* family proteins play important roles in plant stress responses [55, 56]. The *bHLH61* gene in Arabidopsis thaliana was characterized as a negative regulator in response to salt and drought stress [57]. Under salt stress, sorghum inhibited ABA and growth hormone signaling pathways by down-regulating *SbbHLH85*, which appropriately reduced the number and length of root hairs, decreased Na^+ uptake by the root system, and improved resistance to salt stress [58]. *bHLH153* may act as a negative regulator in response to salt stress. Under salt stress, *HD96-1* resisted salt stress by down-regulating *bHLH153* gene expression, but the exact regulatory mechanism is not clear and still needs to be further explored [57].

Under salt stress, *LOC4333197* (*ZFP36*) was significantly down-regulated 32.86-fold in *IR29* (Supplementary table: S15) and up-regulated 3.8-fold in *HD96-1*. This gene belongs to the *C2H2* transcription factors. The *C2H2* zinc finger protein (*ZFP*) gene family plays important roles in plant responses to abiotic and biotic stresses, plant growth and development, and hormone signaling [59, 60]. Expression of zinc finger proteins in Arabidopsis thaliana enhances plant adaptation to salt stress and the proportion of green cotyledons under salt stress conditions [61]. *HD96-1* improves its own salt tolerance by increasing *ZFP36* gene expression under salt stress, which may also be one of the reasons why *HD96-1* is more salt-tolerant than *IR29*. But the exact regulatory mechanism is not clear and still needs to be further explored.

Effect of salt stress on the osmoregulation of rice

Salt stress can cause osmotic stress in plant cells [62]. Many plants can maintain a stable osmotic pressure through solutes that can be fused to each other and protect proteins from degradation through osmoregulation [8]. The control genes related to branched-chain amino acid aminotransferase 2 and branched-chain amino acid aminotransferase 4 in the valine, leucine, and isoleucine pathways were significantly up-regulated under salt stress in both *IR29* and *HD96-1*, and the content of isoleucine was significantly elevated in all of them. Among them, the elevated isoleucine content of *HD96-1* was much higher than that of *IR29*. Branched-chain amino acid transaminase (BCAT) catalyzes the final step in the synthesis of isoleucine [63]. Isoleucine can be used as an osmoprotectant and energy source to alleviate osmotic stress, thereby improving salt tolerance in rice [64]. Physiological results showed that the electrolyte leakage of both *HD96-1* and *IR29* was significantly increased under salt stress, but the amount of change in *HD96-1* was smaller than that in *IR29*. This may be due to the fact that the accumulation of isoleucine in *HD96-1* was more than that in *IR29*, which alleviated osmotic stress, which is in agreement with the previous findings [65]. And this may also be one of the reasons why *HD96-1* was more salt-tolerant.

Salt stress also affects myo-inositol galactosides, raffinose, and stachyose, while many of them have been recognized as osmotic factors in the cytoplasm of plants under salt stress [8]. The related control genes of

galactinol synthase 2 (*LOC4344351*; *OSNPB_070687900*) were significantly up-regulated in both *HD96-1* and *IR29* under salt stress, but the expression was more up-regulated in *HD96-1*. Raffinose family oligosaccharides (*RFOs*) are a family of soluble carbohydrates that are important for plant growth and development and abiotic stress tolerance [66]. Galactinol synthase (*GolS*, EC: 2.4.1.123) is a key enzyme involved in *RFO* biosynthesis [67]. *GolS* transfers galactosyl moieties to myo-inositol to generate galactinol, which forms raffinose and hydrastarch glycosides [68], thereby enhancing its own resistance to salt stress [69]. *HD96-1* significantly up-regulated the relevant control genes of galactoside alcohol synthase 2 (*LOC4344351*; *OSNPB_070687900*) under salt stress, thereby resisting salt stress. This is in agreement with previous studies.

Effect of salt stress on the ionic homeostasis of rice

In plant responses to salt stress, ionic homeostasis such as Na^+ and K^+ is critical for maintaining cytoplasmic enzyme activities, membrane potential, and the proper osmotic pressure of the cell [64]. The Na^+/H^+ antiporters (*NHXs*) play pivotal roles in intracellular Na^+ excretion and vacuolar Na^+ compartmentalization, which are important for plant salt stress resistance [20]. Previous studies have shown that *NHX4* expression in okra was significantly reduced under salt stress, and the results of this experimental study are consistent with the previous study [70]. *IR29* was significantly down-regulated by about 5-fold in the expression of the *LOC9270505* gene (*P0592B08.3*) upon salt stress (Supplementary table: S15), and the expression of the corresponding gene of *HD96-1* did not undergo a significant change. *LOC9270505* belongs to the vesicular membrane *NHX* [71]. Vesicular membrane *NHX* mainly compartmentalizes excess Na^+ in the cytoplasm of the vesicles. We examined the Na^+ content of *IR29* and *HD96-1* after salt stress and found that the sodium content of *HD96-1* was lower compared with *IR29* after salt stress. This may be due to the fact that the expression of the gene controlling the vesicular membrane Na^+/H^+ retrotransporter protein was more stable in *HD96-1* than in *IR29* under salt stress, thus maintaining the function of Na^+ vesicle compartmentalization and preventing excessive accumulation of Na^+, which affects rice growth.

Effect of salt stress on ABA content of rice

The *CYP707A* gene encodes an ABA 8 '-hydroxylase associated with fruit ripening and abiotic stress responses [72]. The catabolic process of abscisic acid is mainly performed by ABA 8'-hydroxylase, which plays an important role in the catabolism of abscisic acid [73]. Silicon has been reported to improve salt resistance by enhancing ABA biosynthesis and water channel protein expression in tobacco [74]. *CYP707A7* (abscisic acid 8'-hydroxylase 3-like; *LOC4347261*) was significantly down-regulated in *HD96-1* and up-regulated in *IR29* under salt stress. By down-regulating *CYP707A7* under salt stress, *HD96-1* might inhibit the activity of ABA 8'-hydroxylase, thus inhibiting the catabolic process of ABA and maintaining the content of ABA to improve the resistance of *HD96-1* to salt stress. However, hormone measurements showed no significant increase in abscisic acid content. This may be due to the fact that ABA content is controlled by a combination of mechanisms [74, 75].

Other genes or metabolites associated with rice resistance to salt stress

The expression of cysteine protease-related control genes (*LOC107280424*, *OSNPB_030752500*) was significantly enhanced in both *HD96-1* and *IR29* after salt stress, but the expression of *HD96-1* was significantly higher than that of *IR29*. Cysteine protease is the most highly induced protease during leaf senescence [76]. When under abiotic stress pressure, cysteine proteases could avoid over consumption of nutrients by accelerating the programmed senescence of some organs in the plant and then transporting them to other organs to ensure the normal growth and development of plants under salt stress [77, 78]. *HD96-1* significantly up-regulated *OSNPB_030752500* expression under salt stress to improve salt tolerance, which is consistent with previous studies.

The control genes related to xyloglucan endotransglucosylase/hydrolase protein 24 (*LOC4341942*, *OSNPB_060696600*) and xyloglucan endotransglucosylase/hydrolase protein 25 (*LOC4341944*, *OSNPB_060697000*) were significantly down-regulated in *HD96-1* and significantly in *IR29* after salt stress up-regulation. As a cell wall-manipulating enzyme, xyloglucan endotransglycosylase/hydrolase (*XTH*) plays an important role in plant resistance to abiotic stresses [79]. In a previous study, it was found that a loss-of-function mutation in Arabidopsis xyloglucan endotransglucosylase-hydrolase30 (*XTH30*) resulted in salt tolerance [80]. In this study, *OSNPB_060696600* and *OSNPB_060697000* acted as negative regulators in response to salt stress. *HD96-1* improves its own salt tolerance by down-regulating the expression of the *OSNPB_060696600* and *OSNPB_060697000* genes, but the specific regulatory mechanism is still unclear and needs to be further explored.

Conclusion

Compared with *IR29*, *HD96-1* showed higher chlorophyll content, photosynthetic efficiency, more stable Na^+/K^+, less H_2O_2, and lower electrolyte leakage under salt stress. Under salt stress, HD96-1 maintained Na^+ and

K^+ homeostasis under salt stress by up-regulating the expression of *NHX4*, mitigated the inhibition of photosynthesis under salt stress by decreasing the accumulation of glucose metabolites, mitigated osmotic stress by increasing the accumulation of isoleucine, and mitigated the oxidative damage induced by salt stress by down-regulating the expression of *ACX4*. *IR29* alleviated salt stress-induced photoinhibition by regulating the absorption of light energy by the light-harvesting chromophore protein complex (LHCH II), thereby improving photosynthetic efficiency under salt stress. In this study, we elucidated the intrinsic molecular mechanisms of salt-tolerant wild rice *HD96-1* and salt-sensitive conventional rice *IR29* adapted to salt stress in terms of ion stabilization, photosynthetic efficiency, oxidative stress, and osmotic stress. This study provides a valuable empirical data for further research on improving salt tolerance in rice or breeding new salt-tolerant varieties.

Materials and methods

Experimental materials

Two indica rice types, *IR29* (salt-sensitive) and *HD96-1* (salt-tolerant), with different genotypes were selected as test materials. Germplasm resources were provided by the College of Coastal Agriculture, Guangdong Ocean University.

Experimental design

The potting experiment was conducted in 2020–2021 in a sunny greenhouse at Guangdong Ocean University, Zhanjiang City, Guangdong Province, China. We used natural light as the light source. In the greenhouse, the daytime and nighttime temperatures were 26 ± 2 °C and 22 ± 2 °C, respectively, and the daytime and nighttime duration lengths were 10 h and 14 h, respectively, with a relative humidity of 70% [81]. Fully matured seeds were selected, then disinfected with 2.5% sodium hypochlorite for 15 min, thoroughly rinsed several times with distilled water. The seeds were soaked in distilled water for 24 h and germinated in the dark for 24 h at 30 °C. Subsequently, 65 seeds were evenly sown in plastic pots (19 cm in upper diameter, 14 cm in lower diameter, 17 cm in height, and with holes at the bottom); each pot was filled with about 2 kg of test soil (the volume ratio of latosol to sand was 3:1). The rice was treated when it grew to the stage of one-leaf-one-heart (1.5 leaf, Day 6 after sowing). A 50 mmol/L NaCl solution was selected to simulate salt stress, and clear water was used as the control. The pots were watered every 3 days with the corresponding concentration of salt solution or clear water, 0.6 L. In order to control the salt concentration of the soil in all treatments of salt stress consistently, the soil salinity was monitored by the Shunkoda soil tester (TR-6D).

The experiment was a completely randomized block design containing two varieties (*IR29* and *HD96-1*) with two treatments each (CK:0 mM NaCl, S: 50 mM NaCl). Each treatment had three biological replicates. (1) ICK: *IR29* conventional control treatment; (2) IS: *IR29* salt stress treatment; (3) HCK: *HD96-1* conventional control treatment; and (4) HS: *HD96-1* salt stress treatment. Samples were taken at the two-leaf-one-heart stage (2.5 leaf, Day 5 after salt stress treatment) and at the four-leaf-one-heart stage (4.5 leaf, Day 18 after salt stress treatment) to determine the morphology of the plants. Physiological samples were cut directly from the leaves of potted plants and stored in liquid nitrogen in a -40 °C freezer for subsequent physiological and biochemical analyses.

Measurement items and methods

Measurement of growth indicators

Plant height and root length were measured with a straightedge; stem base width was measured with vernier calipers; above-ground fresh weight and above-ground dry weight were weighed with a universal balance; leaf area was measured with a leaf area meter (YX-1241); seedlings were cut into above-ground and below-ground portions from the base of the stems and were weighed individually to determine the fresh weights; seedlings were placed in an oven at 105 °C for 30 min, and then dried to a constant weight at 80 °C; aboveground and below-ground portions were measured using a universal balance; and the dry weight of the aboveground and underground parts were measured using a universal balance.

Measurement of photosynthetic gas parameters and chlorophyll fluorescence in rice

Net photosynthetic rate (Pn), intercellular carbon dioxide concentration (Ci), transpiration rate (Tr), and stomatal conductance (Gs) were measured at 9:00–11:00 am on a sunny day with three replicates for each treatment using LI-6400XT. Chlorophyll fluorescence parameters were determined at the 2.5-leaf stage and 4.5-leaf stage using a chlorophyll fluorometer system (OS5P, OPTI-Sciences, USA), and before the determination, Fv/Fm and Fv/F0 were measured and calculated after the dark reaction of rice plants from each treatment for 30 min under dark conditions [82].

Determination of leaf photosynthetic pigment content

Determination of leaf photosynthetic pigment content: 0.1 g of leaves from each treatment was taken at two-leaf-one-heart stage (2.5 leaf) and at the four-leaf-one-heart stage (4.5 leaf), immersed in 10 mL of anhydrous ethanol, and left at room temperature, protected from light for 24 h. The photosynthetic pigment content was

determined by the colorimetric method, and the absorbance values at 665 nm, 649 nm, and 470 nm were determined [83]. The pigment concentration (mg/L) was calculated according to the following formula:

Chlorophyll a (Chl a) = 13.95D665 – 6.88D649.
Chlorophyll b (Chl b) = 24.96D649 – 7.32D665.
Total chlorophyll content = Chl a + Chl b.
Carotenoid (Car) = (1000 D 470 – 2.05 Chl a – 111.48 Chl b)/245.

Measurement of ionic indicators

Na^+ and K^+ contents were measured during the four-leaf-one-heart stage (4.5 leaf) of the rice. The rice shoots were washed with clean water and then dried at 75˚C until attaining a constant weight. the samples were ground into uniform powder using a tissue grinder. 0.2 g sample was weighed and subjected to microwave digestion, ashing and other pretreatments to prepare the liquid to be tested. Na^+ and K^+ contents were determined using an inductively coupled plasma optical emission spectrometer (ICP-OES, Thermo Scientific ICAP 6000 Series).

Determination of membrane damage index

H_2O_2 contents and electrolyte leakage were measured during the two-leaf-one-heart stage (2.5 leaf) and the four-leaf-one-heart stage (4.5 leaf) of the rice. H_2O_2 was determined with reference to the method described by Bates et al. [84]. Electrolyte leakage was determined with reference to the method described by Belkhadi et al. [85].

Extraction and determination of endogenous hormone

A total of 50 mg of the ground sample was weighed, and 10 μL of the internal standard mixing solution at a concentration of 100 mg/mL and 1 mL of methanol/water/formic acid (15:4:1, v/v/v) extractant was added and mixed well; the samples were vortexed for 10 min, and then centrifuged for 5 min at 4 ∘C, 12,000 r/min. And the supernatant was concentrated in a new centrifuge tube. After concentration, the extract was reconstituted with 100 μL of 80% methanol/water solution, passed through a 0.22 μm filter membrane, and put into the injection bottle for LC-MS/MS analysis. Data acquisition was performed using ultra-performance Performance Liquid Chromatography (UPLC) [86]. A MWDB (Metware Database v5.0) database was constructed based on the standards to qualitatively analyze the data detected by mass spectrometry. The quantification was accomplished by analysis using the Multiple Reaction Monitoring (MRM) mode of triple quadrupole mass spectrometry. Analyst 1.6.3 software was used to process the mass spectrometry data. There were three biological replicates for each treatment.

Total RNA isolation and transcriptome analysis

IR29 and *HD96-1* were selected as experimental rice, and the penultimate fully expanded leaf of rice from CK treatment and S treatment was sampled after the 24 h of the end of all treatments, with three biological replications for each treatment. In this experiment, RNA was extracted from rice leaves by ethanol precipitation using the CTAB-PBIOZOL reagent. Total RNA was analyzed qualitatively and quantitatively using a Drop and Agilent 2100 Bioanalyzer (Thermo Fisher Scientific, MA, USA) [87]. Clean reads were obtained using SOAPnuke [88]. The clean reads were then compared to the reference gene sequences using Bowtie2 to obtain the comparison results. Differentially expressed genes with $|\text{Log2FC} \geq 1|$, $P < 0.05$ were screened using Phyper and analyzed by KEGG.

Real-time fluorescence quantitative PCR (qRT-PCR) validation

In order to verify the reliability of the RNA sequencing data, real-time fluorescence quantitative polymerase chain reaction (RT-qPCR) was used for the expression of seven randomly selected differentially expressed genes in the transcriptome and the internal reference gene UBQ5. There were three biological replicates (Supplementary table: S1) for each gene.

Metabolite extraction

The same materials were used for metabolite analysis and the transcriptome. Three replicates were processed for each sample. Each sample was placed in an Eppendorf tube after grinding at 50 Hz for 5 min with a tissue grinder (JXFSTPRP) and ultrasonicated in a water bath at 4 °C for 30 min, followed by refrigeration at -20 °C for one hour. The samples were then centrifuged for 15 min (14,000 RPM Centrifuge Centrifuge (5430)) using a 0.22 m μ membrane filter following LC-MS analysis. In this project, the LC-MS/MS technology was used for non-targeted metabolomics analysis, and the raw mass spectrometry data (raw files) were collected using LC-MS/MS and imported into Compound Discoverer 3.1 (Thermo Fisher Scientific, USA) for data processing, as well as the Metabolome Information Analysis Process for data preprocessing, statistical analysis, metabolite classification annotation, and functional annotation. Three biological replicates for each treatment.

Statistical analysis

Means and standard deviations were calculated using IBM SPSS Statistics 26, and a one-way analysis of variance (ANOVA) was performed. This was followed by Duncan's multiple-range test. $p < 0.05$ was considered a significant difference. Graphs were plotted in the year 2021.

Supplementary Information

The online version contains supplementary material available at https://doi.org/10.1186/s12870-025-06300-8 .

Supplementary Material 1

Supplementary Material 2

Supplementary Material 3

Supplementary Material 4

Acknowledgements
Not applicable.

Author contributions
R.D. Responsible for manuscript writing, investigation, data collation and formal analysis. Y.L. Contributed to the investigation and methods. N.F. Contributed to methodology and conceptualization. D.Z. helps conceptualize, obtain funding, manage and supervise projects. Aaqil Khan Assist in writing censorship and editing. Y.D. Assist in writing censorship and editing. J.Z. Assist in investigation. Z.S. Assist in investigation. J.W. Assist in investigation. Y.X. Assist in investigation. Z.H. Assist in investigation. The police took part in the investigation. All the authors participated in the preparation, writing and revision of the manuscript and adopted the submitted manuscript.

Funding
Guangdong Provincial Education Department Key Field Special Project for Colleges and Universities, No.2021ZdZX4027; Innovation Team Project of Universities in Guangdong Province, No.2021KCXTD011; Binhai Agricultural Engineering Technology Research Center (230420020). Guangdong Ocean University Scientific Research Initiation Project (R20046; 060302052012).

Data availability
The Transcriptome and metabolome data presented in this study can be found in online repositories. The raw sequence data have been deposited in the Genome Sequence Archive in National Genomics Data Center, Beijing Institute of Genomics, Chinese Academy of Sciences, under accession number CRA016731 that are publicly accessible at https://bigd.big.ac.cn/gsa. The metabolite data have been deposited in the National Genomics Data Center, Beijing Institute of Genomics, Chinese Academy of Sciences, under accession number OMIX006554 that are publicly accessible at: https://bigd.big.ac.cn/omix.

Declarations

Ethics approval and consent to participate
Not applicable. All experimental studies on plants were complied with relevant institutional, national, and international guidelines and legislation.

Consent for publication
Not applicable.

Competing interests
The authors declare no competing interests.

Author details
[1]College of Coastal Agriculture Sciences, Guangdong Ocean University, Zhanjiang 524088, China
[2]South China Center of National Saline-tolerant Rice Technology Innovation Center, Zhanjiang 524088, China
[3]Shenzhen Research Institute of Guangdong Ocean University, Shenzhen 518108, China

Received: 13 August 2024 / Accepted: 25 February 2025
Published online: 15 March 2025

References

1. Khan Z, Jan R, Asif S, Farooq M, Jang Y-H, Kim E-G, Kim N, Kim K-M. Exogenous melatonin induces salt and drought stress tolerance in rice by promoting plant growth and defense system. Sci Rep. 2024;14(1):1214.
2. Geng G, Lv C, Stevanato P, Li R, Liu H, Yu L, Wang Y. Transcriptome analysis of salt-sensitive and tolerant genotypes reveals salt-tolerance metabolic pathways in sugar beet. Int J Mol Sci. 2019;20(23):5910.
3. Balasubramaniam T, Shen G, Esmaeili N, Zhang H. Plants' response mechanisms to salinity stress. Plants. 2023;12(12):2253.
4. Ondrasek G, Rathod S, Manohara KK, Gireesh C, Anantha MS, Sakhare AS, Parmar B, Yadav BK, Bandumula N, Raihan F. Salt stress in plants and mitigation approaches. Plants. 2022;11(6):717.
5. Rajabi Dehnavi A, Zahedi M, Piernik A. Understanding salinity stress responses in sorghum: exploring genotype variability and salt tolerance mechanisms. Front Plant Sci. 2024;14:1296286.
6. Wang J, Li Y, Wang Y, Du F, Zhang Y, Yin M, Zhao X, Xu J, Yang Y, Wang W. Transcriptome and metabolome analyses reveal complex molecular mechanisms involved in the salt tolerance of rice induced by exogenous Allantoin. Antioxidants. 2022;11(10):2045.
7. Wang J, Lv J, Liu Z, Liu Y, Song J, Ma Y, Ou L, Zhang X, Liang C, Wang F. Integration of transcriptomics and metabolomics for pepper (Capsicum annuum L.) in response to heat stress. Int J Mol Sci. 2019;20(20):5042.
8. Zhang Y, Li D, Zhou R, Wang X, Dossa K, Wang L, Zhang Y, Yu J, Gong H, Zhang X. Transcriptome and metabolome analyses of two contrasting Sesame genotypes reveal the crucial biological pathways involved in rapid adaptive response to salt stress. BMC Plant Biol. 2019;19:1–14.
9. Yu J, Li P, Tu S, Feng N, Chang L, Niu Q. Integrated analysis of the transcriptome and metabolome of Brassica rapa revealed regulatory mechanism under heat stress. Int J Mol Sci. 2023;24(18):13993.
10. Liu X, Wei R, Tian M, Liu J, Ruan Y, Sun C, Liu C. Combined transcriptome and metabolome profiling provide insights into cold responses in rapeseed (Brassica Napus L.) genotypes with contrasting cold-stress sensitivity. Int J Mol Sci. 2022;23(21):13546.
11. Han C, Chen G, Zheng D, Feng N. Transcriptomic and metabolomic analyses reveal that ABA increases the salt tolerance of rice significantly correlated with jasmonic acid biosynthesis and flavonoid biosynthesis. Sci Rep. 2023;13(1):20365.
12. Fang X, Mo J, Zhou H, Shen X, Xie Y, Xu J, Yang S. Comparative transcriptome analysis of gene responses of salt-tolerant and salt-sensitive rice cultivars to salt stress. Sci Rep. 2023;13(1):19065.
13. Wang X, Wang W, Huang J, Peng S, Xiong D. Diffusional conductance to CO2 is the key limitation to photosynthesis in salt-stressed leaves of rice (Oryza sativa). Physiol Plant. 2018;163(1):45–58.
14. Ling F, Su Q, Jiang H, Cui J, He X, Wu Z, Zhang Z, Liu J, Zhao Y. Effects of Strigolactone on photosynthetic and physiological characteristics in salt-stressed rice seedlings. Sci Rep. 2020;10(1):6183.
15. Zhang R, Wang Y, Hussain S, Yang S, Li R, Liu S, Chen Y, Wei H, Dai Q, Hou H. Study on the effect of salt stress on yield and grain quality among different rice varieties. Front Plant Sci. 2022;13:918460.
16. Zheng C, Liu C, Liu L, Tan Y, Sheng X, Yu D, Sun Z, Sun X, Chen J, Yuan D. Effect of salinity stress on rice yield and grain quality: A meta-analysis. Eur J Agron. 2023;144:126765.
17. Mbarki S, Sytar O, Cerda A, Zivcak M, Rastogi A, He X, Zoghlami A, Abdelly C, Brestic M. Strategies to mitigate the salt stress effects on photosynthetic apparatus and productivity of crop plants. *Salinity responses and tolerance in plants, 1: targeting sensory*. Transp Signal Mech 2018, 85–136.
18. Liu X, Cai S, Wang G, Wang F, Dong F, Mak M, Holford P, Ji J, Salih A, Zhou M. Halophytic NHXs confer salt tolerance by altering cytosolic and vacuolar K + and Na + in Arabidopsis root cell. Plant Growth Regul. 2017;82:333–51.
19. Farooq M, Park J-R, Jang Y-H, Kim E-G, Kim K-M. Rice cultivars under salt stress show differential expression of genes related to the regulation of Na+/K + balance. Front Plant Sci. 2021;12:680131.
20. Cui J-q, Hua Y-p, Zhou T, Liu Y, Huang J-y, Yue C. Global landscapes of the Na+/H + antiporter (NHX) family members uncover their potential roles in regulating the rapeseed resistance to salt stress. Int J Mol Sci. 2020;21(10):3429.
21. Yang Y, Xie J, Li J, Zhang J, Zhang X, Yao Y, Wang C, Niu T, Bakpa EP. Trehalose alleviates salt tolerance by improving photosynthetic performance and maintaining mineral ion homeostasis in tomato plants. Front Plant Sci. 2022;13:974507.
22. Ashraf M. Biotechnological approach of improving plant salt tolerance using antioxidants as markers. Biotechnol Adv 2008.

23. Yan K, Wu C, Zhang L, Chen X. Contrasting photosynthesis and photoinhibition in tetraploid and its autodiploid honeysuckle (Lonicera Japonica Thunb.) under salt stress. Front Plant Sci. 2015;6:227.
24. Joshi S, Nath J, Singh AK, Pareek A, Joshi R. Ion transporters and their regulatory signal transduction mechanisms for salinity tolerance in plants. Physiol Plant 2022, 174 (3), e13702.
25. Yang S, Liu M, Chu N, Chen G, Wang P, Mo J, Guo H, Xu J, Zhou H. Combined transcriptome and metabolome reveal glutathione metabolism plays a critical role in resistance to salinity in rice landraces HD961. Front Plant Sci. 2022;13:952595.
26. Cao L, Zou J, Qin B, Bei S, Ma W, Yan B, Jin X, Zhang Y. Response of exogenous melatonin on transcription and metabolism of soybean under drought stress. Physiol Plant 2023, 175 (5), e14038.
27. Li Y, Tian Q, Wang Z, Li J, Liu S, Chang R, Chen H, Liu G. Integrated analysis of transcriptomics and metabolomics of Peach under cold stress. Front Plant Sci. 2023;14:1153902.
28. Yan G, Fan X, Zheng W, Gao Z, Yin C, Li T, Liang Y. Silicon alleviates salt stress-induced potassium deficiency by promoting potassium uptake and translocation in rice (Oryza sativa L). J Plant Physiol. 2021;258:153379.
29. Khalil R, Yusuf M, Bassuony F, Haroun S, Gamal A. Alpha-tocopherol reinforce selenium efficiency to ameliorates salt stress in maize plants through carbon metabolism, enhanced photosynthetic pigments and ion uptake. South Afr J Bot. 2022;144:1–9.
30. Wang Y, Wang J, Guo D, Zhang H, Che Y, Li Y, Tian B, Wang Z, Sun G, Zhang H. Physiological and comparative transcriptome analysis of leaf response and physiological adaption to saline alkali stress across pH values in alfalfa (Medicago sativa). Plant Physiol Biochem. 2021;167:140–52.
31. Qin C, Ahanger M, Zhou J, Ahmed N, Wei C, Yuan S, Ashraf M, Zhang L. Beneficial role of acetylcholine in chlorophyll metabolism and photosynthetic gas exchange in Nicotiana benthamiana seedlings under salinity stress. Plant Biol. 2020;22(3):357–65.
32. He W, Yan K, Zhang Y, Bian L, Mei H, Han G. Contrasting photosynthesis, photoinhibition and oxidative damage in honeysuckle (Lonicera Japonica Thunb.) under iso-osmotic salt and drought stresses. Environ Exp Bot. 2021;182:104313.
33. Zhang M, Shen J, Wu Y, Zhang X, Zhao Z, Wang J, Cheng T, Zhang Q, Pan H. Comparative transcriptome analysis identified ChlH and POLGAMMA2 in regulating yellow-leaf coloration in Forsythia. Front Plant Sci. 2022;13:1009575.
34. Paddock T, Lima D, Mason ME, Apel K, Armstrong GA. Arabidopsis light-dependent protochlorophyllide oxidoreductase A (PORA) is essential for normal plant growth and development. Plant Mol Biol. 2012;78:447–60.
35. Sun M, Shen Y. Integrating the multiple functions of CHLH into chloroplast-derived signaling fundamental to plant development and adaptation as well as fruit ripening. Plant Sci. 2024;338:111892.
36. Paddock TN, Mason ME, Lima DF, Armstrong GA. Arabidopsis protochlorophyllide oxidoreductase A (PORA) restores bulk chlorophyll synthesis and normal development to a PorB PorC double mutant. Plant Mol Biol. 2010;72:445–57.
37. Wang H, Liu Z, Luo S, Li J, Zhang J, Li L, Xie J. 5-Aminolevulinic acid and hydrogen sulphide alleviate chilling stress in pepper (Capsicum annuum L.) seedlings by enhancing chlorophyll synthesis pathway. Plant Physiol Biochem. 2021;167:567–76.
38. Bambach N, Gilbert ME. A dynamic model of RuBP-regeneration limited photosynthesis accounting for photoinhibition, heat and water stress. Agric for Meteorol. 2020;285:107911.
39. Zhao S, Gao H, Luo J, Wang H, Dong Q, Wang Y, Yang K, Mao K, Ma F. Genome-wide analysis of the light-harvesting chlorophyll a/b-binding gene family in Apple (Malus domestica) and functional characterization of MdLhcb4. 3, which confers tolerance to drought and osmotic stress. Plant Physiol Biochem. 2020;154:517–29.
40. Saccon F, Durchan M, Bína D, Duffy CD, Ruban AV, Polívka T. A protein environment-modulated energy dissipation channel in LHCII antenna complex. Iscience 2020, *23* (9).
41. Lu X, Ma L, Zhang C, Yan H, Bao J, Gong M, Wang W, Li S, Ma S, Chen B. Grapevine (Vitis vinifera) responses to salt stress and alkali stress: transcriptional and metabolic profiling. BMC Plant Biol 2022.
42. Lu X, Ma L, Zhang C, Yan H, Bao J, Gong M, Wang W, Li S, Ma S, Chen B. Grapevine (Vitis vinifera) responses to salt stress and alkali stress: transcriptional and metabolic profiling. BMC Plant Biol. 2022;22(1):528.
43. Peng X, Deng X, Tang X, Tan T, Zhang D, Liu B, Lin H. Involvement of Lhcb6 and Lhcb5 in photosynthesis regulation in Physcomitrella patens response to abiotic stress. Int J Mol Sci. 2019;20(15):3665.
44. Li H, He X, Gao Y, Liu W, Song J, Zhang J. Integrative analysis of transcriptome, proteome, and phosphoproteome reveals potential roles of photosynthesis antenna proteins in response to brassinosteroids signaling in maize. Plants. 2023;12(6):1290.
45. Roth MS, Westcott DJ, Iwai M, Niyogi KK. Hexokinase is necessary for glucose-mediated photosynthesis repression and lipid accumulation in a green Alga. Commun Biology. 2019;2(1):347.
46. Deng R, Zheng D, Feng N, Khan A, Zhang J, Sun Z, Li J, Xiong J, Ding L, Yang X, et al. Prohexadione calcium improves rice yield under salt stress by regulating Source–Sink relationships during the filling period. Plants. 2025;14(2):211.
47. Sehar Z, Iqbal N, Khan M, Masood A, Rehman T, Hussain A, Khan N. Ethylene reduces glucose sensitivity and reverses photosynthetic repression through optimization of glutathione production in salt-stressed wheat (Triticum aestivum L). Sci Rep. 2021;11:12650.
48. Siddiqui H, Sami F, Bajguz A, Hayat S. Glucose escalates PSII activity, dynamics between anabolic and catabolic pathways, redox and elemental status to promote the growth of Brassica juncea. South Afr J Bot. 2021;137:68–84.
49. Baba SA, Vishwakarma RA, Ashraf N. Functional characterization of CsBGlu12, a beta-glucosidase from Crocus sativus provides insights into its role in abiotic stress through accumulation of antioxidant flavonols. J Biol Chem 2017.
50. Salgado JCS, Meleiro LP, Carli S, Ward RJ. Glucose tolerant and glucose stimulated β-glucosidases – A review. Bioresour Technol 2018.
51. Wang Y, Zhao H, Qin H, Li Z, Liu H, Wang J, Zhang H, Quan R, Huang R, Zhang Z. The synthesis of ascorbic acid in rice roots plays an important role in the salt tolerance of rice by scavenging ROS. Int J Mol Sci. 2018;19(11):3347.
52. Chen XF, Tian MX, Sun RQ, Zhang ML, Zhou LS, Jin L, Chen LL, Zhou WJ, Duan KL, Chen YJ. SIRT 5 inhibits peroxisomal ACOX 1 to prevent oxidative damage and is downregulated in liver cancer. EMBO Rep 2018, 19 (5), e45124.
53. Song HongMiao SH, Zhao RongMin ZR, Fan PengXiang FP, Wang XuChu WX, Chen XianYang CX, Li. YinXin, L. Y. Overexpression of AtHsp90. 2, AtHsp90. 5 and AtHsp90. 7 in Arabidopsis thaliana enhances plant sensitivity to salt and drought stresses. 2009.
54. Shen M, Cai R, Li Z, Chen X, Xie J. The molecular mechanism of Yam polysaccharide protected H2O2-Induced oxidative damage in IEC-6 cells. Foods. 2023;12(2):262.
55. Liang X, Li Y, Yao A, Liu W, Yang T, Zhao M, Zhang B, Han D. Overexpression of MxbHLH18 increased iron and high salinity stress tolerance in Arabidopsis thaliana. Int J Mol Sci. 2022;23(14):8007.
56. Alabd A, Cheng H, Ahmad M, Wu X, Peng L, Wang L, Yang S, Bai S, Ni J, Teng Y. ABRE-BINDING FACTOR3-WRKY DNA-BINDING PROTEIN44 module promotes salinity-induced malate accumulation in Pear. Plant Physiol. 2023;192(3):1982–96.
57. Wang Y, Fang Z, Yang L, Chan Z. Transcriptional variation analysis of Arabidopsis ecotypes in response to drought and salt stresses dissects commonly regulated networks. Physiol Plant. 2021;172(1):77–90.
58. Song Y, Li S, Sui Y, Zheng H, Han G, Sun X, Yang W, Wang H, Zhuang K, Kong F. SbbHLH85, a bHLH member, modulates resilience to salt stress by regulating root hair growth in sorghum. Theor Appl Genet 2022, 1–16.
59. Li Y, Chu Z, Luo J, Zhou Y, Cai Y, Lu Y, Xia J, Kuang H, Ye Z, Ouyang B. The C2H2 zinc-finger protein SI ZF 3 regulates AsA synthesis and salt tolerance by interacting with CSN 5B. Plant Biotechnol J. 2018;16(6):1201–13.
60. Jiang Y, Liu L, Pan Z, Zhao M, Zhu L, Han Y, Li L, Wang Y, Wang K, Liu S. Genome-wide analysis of the C2H2 zinc finger protein gene family and its response to salt stress in ginseng, Panax ginseng Meyer. Sci Rep. 2022;12(1):10165.
61. Teng K, Tan P, Guo W, Yue Y, Fan X, Wu J. Heterologous expression of a novel Zoysia japonica C2H2 zinc finger gene, ZjZFN1, improved salt tolerance in Arabidopsis. Front Plant Sci. 2018;9:1159.
62. Kawa D, Testerink C. Regulation of mRNA decay in plant responses to salt and osmotic stress. Cell Mol Life Sci. 2017;74(7):1165–76.
63. Diebold R, Schuster J, Däschner K, Binder S. The branched-chain amino acid transaminase gene family in Arabidopsis encodes plastid and mitochondrial proteins. Plant Physiol. 2002;129(2):540–50.
64. Hacham Y, Shitrit O, Nisimi O, Friebach M, Amir R. Elucidating the importance of the catabolic enzyme, methionine-gamma-lyase, in stresses during Arabidopsis seed development and germination. Front Plant Sci. 2023;14:1143021.
65. Wu K, Liang X, Zhang X, Yang G, Wang H, Xia Y, Ishfaq S, Ji H, Qi Y, Guo W. Metabolomics analysis reveals enhanced salt tolerance in maize through exogenous Valine-Threonine-Isoleucine-Aspartic acid application. Front Plant Sci. 2024;15:1374142.

66. De Koning R, Wils GE, Kiekens R, De Vuyst L, Angenon G. Impact of drought and salt stress on galactinol and raffinose family oligosaccharides in common bean (Phaseolus vulgaris). AoB Plants. 2023;15(4):plad038.
67. Jing Q, Chen A, Lv Z, Dong Z, Wang L, Meng X, Feng Y, Wan Y, Su C, Cui Y. Systematic analysis of galactinol synthase and raffinose synthase gene families in potato and their expression patterns in development and abiotic stress responses. Genes. 2023;14(7):1344.
68. Ranjan A, Gautam S, Michael R, Shukla T, Trivedi PK. Arsenic-induced galactinol synthase1 gene, AtGolS1, provides arsenic stress tolerance in Arabidopsis thaliana. Environ Exp Bot. 2023;207:105217.
69. Li H, Di Gao Y, Kang LQ, Yu HY, Zeng LM, Wang YH, Chen RR, Song JB. Identification of the galactinol synthase (GolS) family in Medicago truncatula and expression analysis under abiotic stress and phytohormone treatment. J Plant Growth Regul 2024, 1–14.
70. Yousefi K, Jamei R, Darvishzadeh R. Exogenous 24-Epibrassinolide alleviates salt stress in Okra (Abelmoschus esculentus L.) by increasing the expression of SOS pathway genes (SOS1-3) and NHX1, 4. Physiol Mol Biology Plants 2024, 1–13.
71. Sellamuthu G, Jegadeeson V, Sajeevan RS, Rajakani R, Parthasarathy P, Raju K, Shabala L, Chen Z-H, Zhou M, Sowdhamini R. Distinct evolutionary origins of intron retention splicing events in NHX1 antiporter transcripts relate to sequence specific distinctions in Oryza species. Front Plant Sci. 2020;11:267.
72. Cai Y, Zhu P, Liu C, Zhao A, Yu J, Wang C, Li Z, Huang P, Yu M. Characterization and expression analysis of cDNAs encoding abscisic acid 8′-hydroxylase during mulberry fruit maturation and under stress conditions. Plant Cell Tissue Organ Cult (PCTOC). 2016;127:237–49.
73. Okazaki M, Kittikorn M, Ueno K, Mizutani M, Hirai N, Kondo S, Ohnishi T, Todoroki Y. Abscinazole-E2B, a practical and selective inhibitor of ABA 8′-hydroxylase CYP707A. Bioorg Med Chem. 2012;20(10):3162–72.
74. Liu X, Niu H, Li J, Jiang D, Chen R, Zhang R, Li Q. Higher endogenous abscisic acid confers greater tolerance to saline-alkaline stress in Petunia hybrida. Environ Exp Bot 2024, 106035.
75. Chen H, Liu X, Mao J, Qi X, Chen S, Feng J, Jin Y, Ahmad MZ, Sun M, Deng Y. Comparative transcriptomic and physiological analyses reveal the key role of abscisic acid in hydrangea macrophylla responding to Corynespora Cassiicola. BMC Plant Biol. 2024;24(1):1–15.
76. James M, Poret M, Masclaux-Daubresse C, Marmagne A, Coquet L, Jouenne T, Chan P, Trouverie J, Etienne P. SAG12, a major cysteine protease involved in nitrogen allocation during senescence for seed production in Arabidopsis thaliana. Plant Cell Physiol. 2018;59(10):2052–63.
77. Miryeganeh M. Epigenetic mechanisms of senescence in plants. Cells. 2022;11(2):251.
78. Guiboileau A, Sormani R, Meyer C, Masclaux-Daubresse C. Senescence and death of plant organs: nutrient recycling and developmental regulation. CR Biol. 2010;333(4):382–91.
79. Yan J, Huang Y, He H, Han T, Di P, Sechet J, Fang L, Liang Y, Scheller HV, Mortimer JC. Xyloglucan endotransglucosylase-hydrolase30 negatively affects salt tolerance in Arabidopsis. J Exp Bot. 2019;70(19):5495–506.
80. Tiika RJ, Wei J, Cui G, Ma Y, Yang H, Duan H. Transcriptome-wide characterization and functional analysis of Xyloglucan endo-transglycosylase/hydrolase (XTH) gene family of Salicornia europaea L. under salinity and drought stress. BMC Plant Biol. 2021;21:1–15.
81. Zhao H-M, Zheng D-F, Feng N-J, Zhou G-S, Khan A, Lu X-T, Deng P, Zhou H, Du Y-W. Regulatory effects of Hemin on prevention and rescue of salt stress in rapeseed (Brassica Napus L.) seedlings. BMC Plant Biol. 2023;23(1):558.
82. Chen J, Wu F-H, Wang W-H, Zheng C-J, Lin G-H, Dong X-J, He J-X, Pei Z-M, Zheng H-L. Hydrogen sulphide enhances photosynthesis through promoting Chloroplast biogenesis, photosynthetic enzyme expression, and thiol redox modification in Spinacia oleracea seedlings. J Exp Bot. 2011;62(13):4481–93.
83. Lichtenthaler HK, [34]. Chlorophylls and carotenoids: pigments of photosynthetic biomembranes. Methods in enzymology. Volume 148. Elsevier; 1987. pp. 350–82.
84. Hussain SJ, Masood A, Anjum NA, Khan NA. Sulfur-mediated control of salinity impact on photosynthesis and growth in Mungbean cultivars screened for salt tolerance involves glutathione and proline metabolism, and glucose sensitivity. Acta Physiol Plant. 2019;41:1–13.
85. Belkhadi A, Hediji H, Abbes Z, Nouairi I, Barhoumi Z, Zarrouk M, Chaïbi W, Djebali W. Effects of exogenous Salicylic acid pre-treatment on cadmium toxicity and leaf lipid content in Linum usitatissimum L. Ecotoxicol Environ Saf. 2010;73(5):1004–11.
86. Pan X, Welti R, Wang X. Quantitative analysis of major plant hormones in crude plant extracts by high-performance liquid chromatography–mass spectrometry. Nat Protoc. 2010;5(6):986–92.
87. Fan M, Tang X, Yang Z, Wang J, Zhang X, Yan X, Li P, Xu N, Liao Z. Integration of the transcriptome and proteome provides insights into the mechanism calcium regulated of Ulva prolifera in response to high-temperature stress. Aquaculture. 2022;557:738344.
88. Li R, Li Y, Kristiansen K, Wang J. SOAP: short oligonucleotide alignment program. Bioinformatics. 2008;24(5):713–4.

Publisher's note